Supplementary Online Content

Beltran H, Eng K, Mosquera JM, et al. Whole-exome sequencing of metastatic cancer and biomarkers of treatment response. *JAMA Oncol*. Published online May 28, 2015. doi:10.1001/jamaoncol.2015.1313

This supplementary material has been provided by the authors to give readers additional information about their work.

eMethods

Patient enrollment and tumor acquisition. All patients signed informed consent under an Institutional Review Board (IRB) approved protocol (IRB #1305013903), and tumor specimens were obtained prospectively or retrospectively (IRB #1305013903, #1007011157; #1210013164A005). All fresh/frozen tissues were processed immediately after surgical procedure or biopsy as outlined in the PM Pathology SOPs **(see eAppendix B).** For solid tumors, hematoxylin and eosin stained slides of both FFPE and frozen tissue blocks were reviewed by one of the study pathologists (JMM, BR, MAR) for tumor purity assessment and selection of high-density areas for manual dissection and DNA extraction.

DNA extraction and next generation sequencing. Genomic DNA was extracted from macrodissected FFPE tumor and/or cored frozen, OCT-embedded tumor, and peripheral blood mononuclear cells using the Promega Maxwell 16 MDx. Estimation of tumor content was based on analysis of the sequencing data using CLONET version 0.3. (1) and by study pathologist's review. At least 200ng of DNA was required to proceed with whole exome sequencing. High DNA quality was confirmed for all samples by a real-time PCR prior to sequencing. Sequencing was performed using Illumina HiSeq 2500 (2x100bp). A total of 21,522 genes were analyzed with an average coverage of 84x (81x) using Agilent HaloPlex Exome. On average, 71,073,768 (68,658,329) short reads are obtained and processed accordingly to IPM-Exome-pipeline v0.9.

.

Data processing and Quality Control. FastQC (http://www.bioinformatics.babraham.ac.uk/projects/fastqc/) is run on the raw reads to assess the quality of the raw reads. The output of FastQC gives several metrics, including the average base quality of the raw reads, the sequence duplication of the raw reads, and the *k*-mer enrichment along the length of the raw reads. We keep these measures to assess whether the sequencing or demultiplexing of the samples was performed correctly. After initial QC, adapter sequences are trimmed using Trimmomatic.

Short reads were then aligned to GRC37/hg19 reference using BWA. The alignment and analysis of the exome data was processed on Sun Grid Engine computing cluster using 8 CPU cores with 16Gb of memory. Under these conditions an exome on average takes ~8-10 hours to align and analyze for genomic alterations. For quality control of the sequencing, alignment, and analysis of our samples, quality control is assessed in three general phases: 1) The quality of the raw reads (see above), 2) The quality of the alignment, 3) The quality of the samples. As an additional quality control paired 'tumor' and 'control' NA12878 samples are sequenced with every batch of samples sequenced. The 'tumor' sample is the NA12878 sample spiked with JAK2 mutation, EGFR deletion, and HER2 amplification. The 'control' NA12878 sample is the canonical NA12878 samples with no spiked JAK2 mutation, EGFR deletion, and HER2 amplification.

The alignment quality of the aligned BAM files is obtained by calculating several metrics related to the average coverage and capture rate by calculating how many aligned reads fall within a capture region in the Agilent HaloPlex Whole Exome kit. Our capture rate is given by the percent of mapped reads found overlapping any capture region in the Agilent HaloPlex Whole Exome kit and the total number of mapped reads of any given sample. High quality capture rates range from ~80-95 %. Average coverage is computed by calculating the average number of reads found overlapping a capture region in the Agilent HaloPlex Whole Exome kit. Typically the average coverage of a sample ranged from 80-100X.

Two items are investigated to assess the quality of the samples: 1) Whether the paired tumor/control samples originate from the same patient and 2) How pure a tumor sample is by calculating a tumor purity estimate derived from the copy number analysis.

In order to surmise whether or not the matched samples originate from the same patient, genotypes of 334 SNPs are computed using Goby(2) and the genotypic distance of these SNPs are calculated for each sample using SPIAssay(3) (https://github.com/cran/SPIAssay), a package in R. These 334 SNPs are chosen such that the genotypes of the 334 SNPs should be very similar in paired tumor/control samples that originate from the same patient versus paired samples that originate from different patient. For a negative control the genotype distance between the paired tumor/control samples with a random sample that originates from a different patient is also computed.

The tumor purity estimate is computed using in-house developed software, CLONET(1, 4). CLONET takes into account the copy number alteration segments (described later in our methods section) and the genotypes of SNPs found within these copy number alteration segments.

Detection of Point mutations and indels. Point mutations are detected through three separate approaches. One pipeline uses an in-house SNV caller, SNVseeqer to determine which point mutations are found primarily in the tumor. Mutations found at positions reported in dbSNP (Build 137) are filtered out. As an additional filter, mutations are kept if they are located in coding sequences and caused an amino acid change determined by SNVseeqer(5). Indels are detected using GATK somatic indel with default parameters. These mutations must be covered by at least 10 aligned reads in the tumor and matched control. Furthermore, the mutations are filtered by variant allele frequency where the mutation has to be present in the tumor with a variant allele frequency > 25% and the present in the matched control with a variant allele frequency < 1%.

A second approach directly interrogates the tumor and matched control at positions reported in COSMIC. COSMIC is a database of somatic cancer mutations curated by the Sanger Institute (http://www.sanger.ac.uk). Positions that were reported more than ten times in the database were interrogated. At each of these positions, Samtools interrogates the aligned reads in the tumor and matched control sample and mutations that have a variant allele frequency >5% in the tumor and <1% in the control are kept. These mutations must be covered by at least 5 aligned reads in both the tumor and control sample. Lastly mutations are filtered out if the Annovar mutation annotation tool does not predict the mutation to cause an amino acid change (based on RefSeq gene annotation).

The third approach complements the second one and uses the same approach to look at the tumor and control at positions where mutations are known a priori to be clinically relevant. These positions are generated through literature and database search and placed in the clinically relevant category if a mutation in a specific genomic region is known to have sensitivity to an FDA approved drug(s). Samtools is used to look at the tumor and matched control sample and report mutations that has a variant allele frequency >5% in the tumor and < 1% in the control(6). Mutations must be covered by at least 5 aligned reads in both the tumor and control sample. Mutations predicted to cause an amino acid change by Annovar are kept. Specific clinical relevant long indels in EGFR and FLT3 (ITD) are detected using PINDEL, a tool that can detect longer indels.

Detection of Somatic Copy number alterations. For somatic copy number alterations the number of aligned reads for capture region in the Agilent HaloPlex Whole Exome Kit was calculated in both the tumor sample and matched control sample. Our rationale for taking this approach is that genomic regions that are aligned more frequently in the tumor sample relative to control sample is indicative of copy number gain. Conversely, genomic regions that are aligned less frequently in the tumor sample relative to control sample is indicative of copy number gain. Capture regions with a total coverage < 100 reads in both the tumor sample and matched control sample are filtered out. For the remaining capture regions, read counts are normalized in both the tumor sample and the matched control sample by the total number of reads aligned in the tumor sample and the matched control sample respectively. Then the ratio of the normalized read counts in the tumor sample and the normalized read count in the control sample is calculated. These capture regions are then ordered karyotypically and sorted by genomic coordinates to help segment our capture regions according to the log2 value of the ratio of normalized read counts of the tumor sample and control sample in a biologically meaningful way. The normalized ratios of these bins was segmented using the Circular Binary Segmentation algorithm implemented in the R package DNAcopy. The algorithm outputs segments where every capture region found within these segments is represented by the same log2 value. This log2 value indicates whether the segment has DNA copy number gain (amplification) or DNA copy number loss (deletion). A negative log2 would suggest a segment was deleted and a positive value would suggest a segment is amplified. Segments with a log2 value > 0.5 to are amplified and segments with a log2 value < -0.5 are categorized as deleted. We then took the segments called by the algorithm and annotated theses segments by RefSeq genes whose transcription start and end sites overlap with the genomic coordinates assigned to these segments.

Mutation categorization. Mutations obtained from all three approaches are merged into a single list using an union strategy. All the mutations are then categorized by category I, category II, and category III. The mutation was categorized as category I if the mutation detected has been previously reported to have sensitivity to an FDA approved drug(s) or if they have clinical relevance. Mutations found within a cancer gene that are not clinically relevant are reported as category II. The list of cancer genes was determined using the Cancer Gene Census from the Trust Sanger Institute. Mutations that could not be categorized as category I or category II are categorized as category III.

EXaCT-1 Sequencing Report. Photomicrographs of tumor histology and any ancillary studies (e.g., immunohistochemistry or FISH results, when applicable) are shown on the report of the specimen sequenced, as well as clinical information including disease type, site of biopsy, and tumor content. Automated lists of Category I-III alterations are populated in the Report and subjected to manual review, with references and clinical trial information included and updated on a continual basis. Additional data sharing with clinicians and team members occurs through an internal web-based cBioPortal for data visualization, a BAM file viewing interface using IGV and integration with EMR systems.

Whole genome sequencing. For this study, whole genome sequencing was performed at Illumina and at the New York Genome Center (NYGC). Paired-end 2x100 reads were aligned to the GRCh37 human reference using the Burrows-Wheeler Aligner (BWA)(7). The mapped reads were processed using Picard tools (http://picard.sourceforge.net) to mark duplicate reads and using the Genome Analysis Toolkit (GATK) [2](8) for realignment around indels and base recalibration. For structural variant (SV) calling we applied Crest(9) which uses soft-clipped reads and local assembly to detect deletions, inversions, inter-/intra-chromosomal translocations, and insertions.

Precision Medicine Tumor Board. We have integrated our PM Tumor Board into fellowship training in medical oncology, pathology, and surgical oncology. Clinical fellows participate in various weekly small group meetings and are trained in data visualization (including direct, regulatory compliant links to the IGV site loaded with the patient's data) and interpretation. After discussion, clinical fellows presents each case including pertinent history, clinical presentation and course, prior therapies, imaging studies, pathology and genomic data at biweekly PM Tumor Board. The fellow reviews published data relating specific mutations and potential response to approved therapies, clinical trial options, as well as novel targets in preclinical or early phase development. These results are discussed amongst a multidisciplinary team including the referring physician, medical oncology, pathology, surgical oncology, computational biology, and basic science. For mutations of unknown clinical or biologic significance, crowd-sourcing approaches help the PM community annotate and prioritize alterations. Powerpoint presentations and one –page tumor board summaries are archived for each case.

FANCA Fluorescence *in situ* hybridization (FISH). *FANCA* gene specific probe (BAC clone RP11-79A1) and a reference probe located at 16p12 (BAC clone RP11-450G5) were used for this approach. Five μm–thick tissue sections were used for FISH analysis. Deletion was defined as presence of only copy of *FANCA* specific probe in the presence of two reference signals, per nucleus. At least 100 nuclei were evaluated per tissue section or 50 nuclei per tissue core in tissue microarrays (TMAs), using a fluorescence microscope (Olympus BX51; Olympus Optical, Tokyo, Japan).

Transfection. Transient transfections of siRNA was performed using 40nM FANCA siRNA (ON-TARGETplus SMARTpool L-019283-00, Thermo Scientific, Waltham, MA) or 40nM control nonsilencing siRNA (ON-TARGETplus Non-targeting Pool D-001810; Thermo Scientific, Waltham, MA). siRNA was introduced into cells using lipofectamine following the manufacturer's protocol. Briefly $4x10^5$ cells were seeded in 6-wells in 2mL medium and transfected with siRNA. Following 48 hours RNA was extracted and quantitative RT-PCR was performed. All experiments were performed in duplicate. Transfection of CRISPR plasmids with either the FANCA target sequence or with empty vector was performed using TransIT-X2 reagent (Mirus Bio, Madison, WI) using manufacturer's protocols. $4x10^5$ 22Rv1 cells were grown in 6 wells in 2.5ml medium and transfected with 2.5□g of plasmid together with 12.5□l of TransIT-X2 (1:5 ratio). Media was changes after 24h and after 72h cells were re-plated in media containing 1□g/ml Puromycin.

CRISPR Mediated Disruption of FANCA Gene in 22Rv1 Cells. The CRISPR/Cas9 plasmid (Px459) was obtained from Addgene (Cambridge, MA). Using Ran *et al*(10) protocol we identified a FANCA CRISPR DNA target sequence using algorithms based on analysis in Hsu *et al*(11). The corresponding oligonucleotides were ordered (IDT Coralville, IA) and were cloned into Px459 vector. Sanger sequencing confirmed integration of the FANCA target site into the vector.

Drug Treatment *in vitro*. Cisplatin was obtained from Sigma P4394. Prostate cell lines for this study were obtained from the American Type Culture Collection (Manassas, VA). We obtained isogenic fibroblast cell line with and without FANCA expression (from AS, Rockefeller University). The indicated cells were seeded on 6-well-tissue culture plates. Cell lines were treated with vehicle (0.1% DMSO) or escalating doses of cisplatin. Following 4 days incubation cells were trypsinized and re-seeded in 96 well plates. Cell viability was assessed using Cell Titer-Glo luminescent assay (Promega Corporation, Madison, WI) as we have previously described (12) according to the manufacturer's instructions. Cell viability dose response data were first normalized to data using the vehicle treated control and then analyzed using nonlinear regression in

which the log(inhibitor) versus normalized response curves were generated and the IC50 doses were calculated (GraphPad Software, San Diego California USA, www.graphpad.com).

Immunofluorescent Labeling of Monolayer cells. Five sterile 12mm circular cover slips were placed in each of the wells of a 6 well dish. FANCA positive or negative cells were plated at a density of $1e^5$ to $2.5e^5$ cells per well. The next day, cells were treated with vehicle or 1uM MMC (Sigma) for 24 hours. Cells were washed twice in PBS. Following incubation in 0.5% TritonX100 (Sigma) for 5min cells were permeabilized in 0.5% NP-40 in PBS for 10min and washed once in PBS. Cover slips with cells were incubated in PBG blocking solution (0.2% w/v cold water fish gelatin (Sigma), 0.5% w/v BSA (sigma) in PBS) for 20 minutes then were incubated in either FANCI or FANCD2 (Novus Bio) primary antibody at a dilution of 1/1000 in PBG at room temperature for two hours. Cells were washed 3 times 5 minutes each in PBG and incubated in secondary antibody (Alexa Fluor 488 Goat anti Rabbit, Life Technologies) at 1/1000 dilution in PBG for one hour at room temperature. Cells were then washed 3 times 5 minutes and cover slips were mounted on slides in ProLong Gold Antifade Mountant with DAPI (Life Technologies). Foci formation was analyzed on an Olympus BX51 under 60x oil objective.

Immunoblot Analysis. Protein lysates were prepared in the RIPA buffer (radioimmunoprecipitation assay lysis buffer) supplemented with protease inhibitor cocktail and phosphatase inhibitors (Thermo Scientific, Waltham, MA). The total protein concentration of the soluble extract was determined using the BCA protein assay Kit (Thermo Scientific). Each protein sample (20ug) was resolved to SDS–PAGE, transferred onto a polyvinylidene difluoride membrane (BioRad) and incubated overnight at 4°C with primary antibodies. The antibodies used were: anti-FANCA (A301-980A, Bethyl Laboratories USA) . Following three washes with TBS-T, the blot was incubated with horseradish peroxidase-conjugated secondary antibody and immune complexes were visualized by enhanced chemiluminescence detection (Luminata Forte WBLUF0500, Millipore, USA). The blot was re-probed with monoclonal antibody against anti-GAPDH (AB2302 Millipore, USA).

Xenografts. Patient derived xenografts were developed in collaboration with the Living Tumor Laboratory, University of British Columbia, as previously described (3). In brief, fresh tumor tissue was sent immediately in organ media to the Living Tumor Laboratory and grafted into the subrenal capsules of NOD SCID mice (NOD.CB17-Prkdcscid/J) within 24 hours. After 3-6 months of growth, the animals were sacrificed and tumors were harvested and regrafted. For drug treatment studies, tumors were allowed to grow to an average tumor volume of 90 mm^3. For each model (LTL545 or LTL352) 10 mice bearing 1-2 tumors each (n = 15 total tumors per model) were randomized to treatment with cisplatin intraperitoneal dosing of vehicle or cisplatin (4mg/kg, day 1 and day 8) for 10-14 days. Body weight, tumor volume based on caliper measurements (0.5236 x length x width) and final tumor weight were assessed. The longitudinally collected tumor sizes were first log-transformed and then analyzed using mixed effects analysis assuming an autoregressive within-mouse correlation structure. Missing data were treated as missing-at-random (MAR). The tumor weights at final day were compared using nonparametric method – Wilcoxon Rank-sum test. All tests are two-sided with a 0.05 level of significance.

Supplementary Figures

eFigure 1. A schematic of the IPM Computational Pipeline

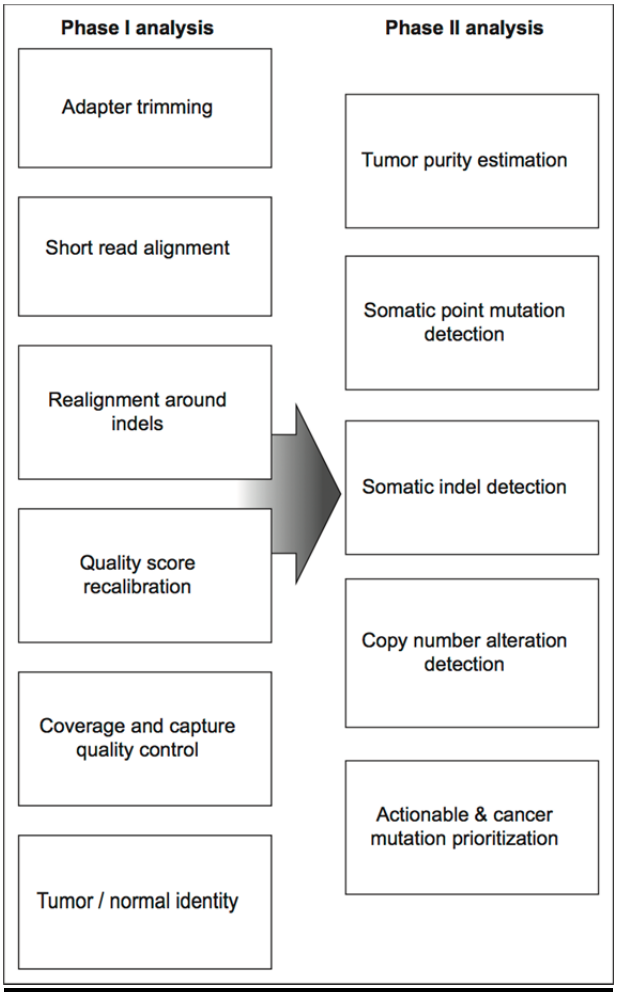

eFigure 2. Tumor purity analysis

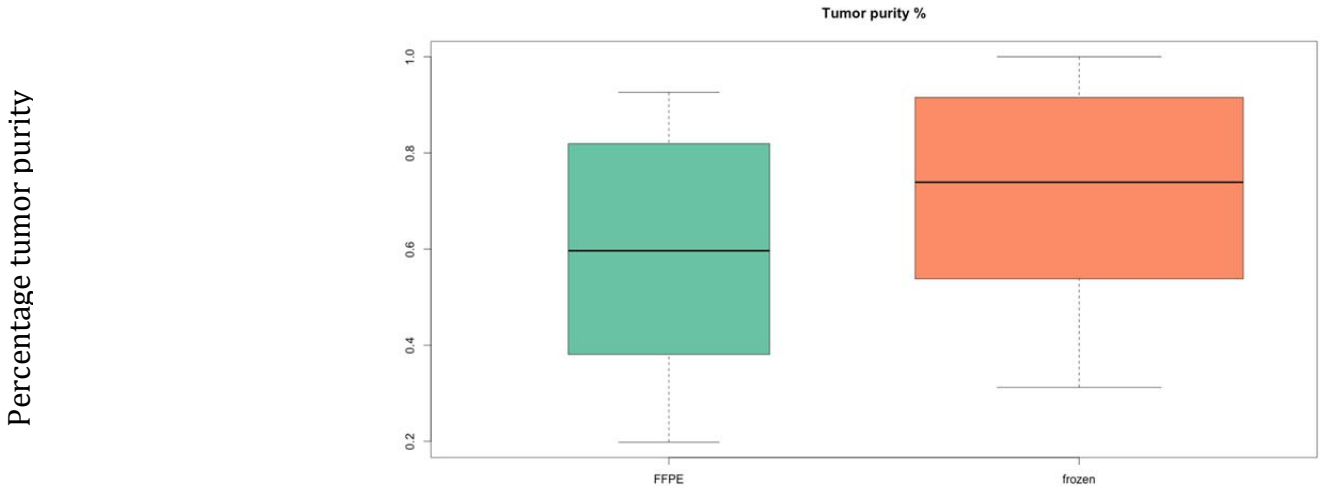

The tumor purity across PM cases ranges from: 14% to 100% with more than 50% of the cases with tumor purity > 25%. This Figure shows distribution of tumor purity by specimen type (frozen vs. FFPE). The difference is significant (p-value = 0.02) with lower tumor content for the FFPE cases. Size of box plots is proportional to the number of cases in each group.

eFigure 3. Tumor purity estimates from Pathology team versus computationally (CLONET) estimated tumor purities values for frozen tumor specimens (Spearman correlation 0.2765327, p-value = 0.03561). The x-axis represents the tumor purity estimates from the pathologists and the y-axis represents tumor purity computed by CLONET.

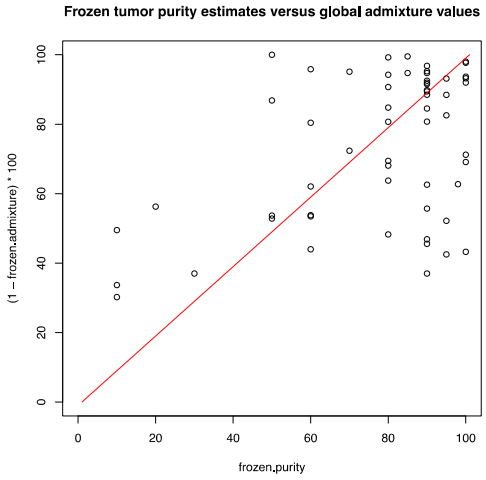

eFigure 4. Sequencing metrics Fresh/frozen vs. FFPE tissue

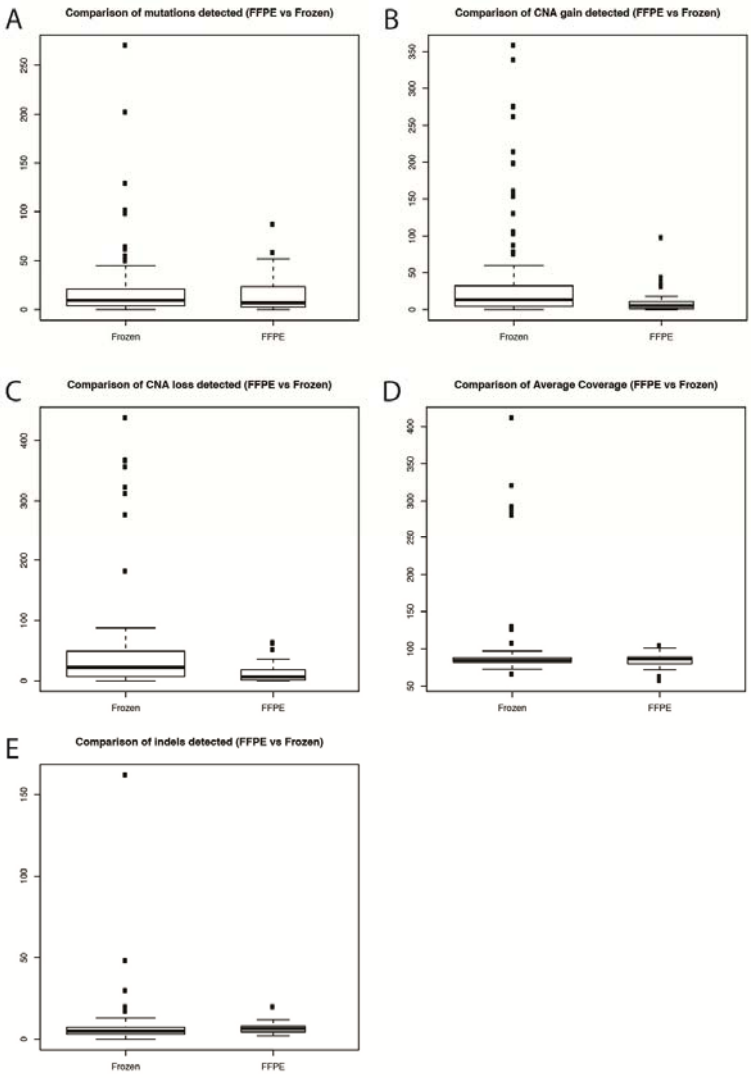

Comparison of mutation rate **(A),** somatic copy number alterations **(B-C),** average coverage **(D)**, and indel detection **(D)** between frozen and FFPE tissue. Y-axis designates the number of alterations.

eFigure 5. Somatic copy number alteration profiles by tumor type at cytogenetic map location resolution; for each cytogenetic map location the mean genes aberration frequency is reported. Frequencies are computed on based on 77 prostate cancer samples, 32 other cancers samples and 34 urothelial cancer samples.

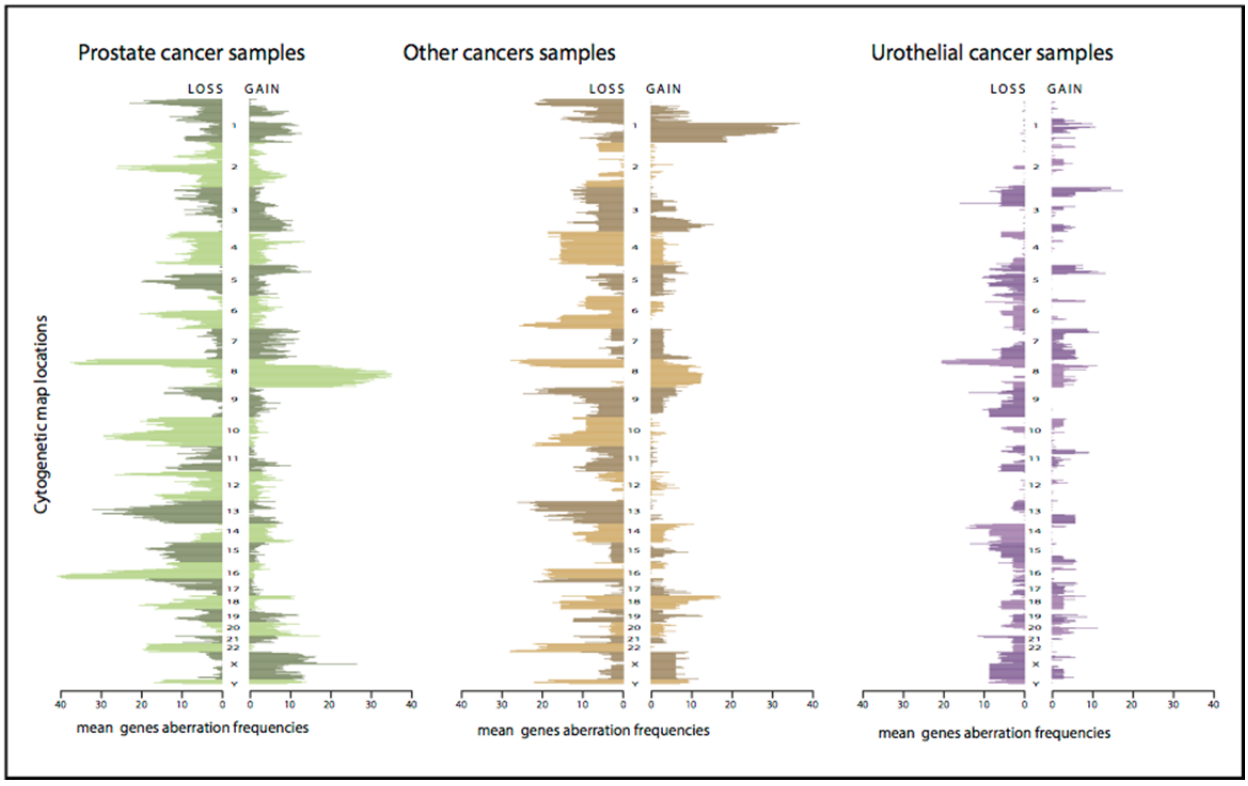

eFigure 6. The 20 most frequently aberrant genes with respect to copy number gains/losses detected per tumor type.

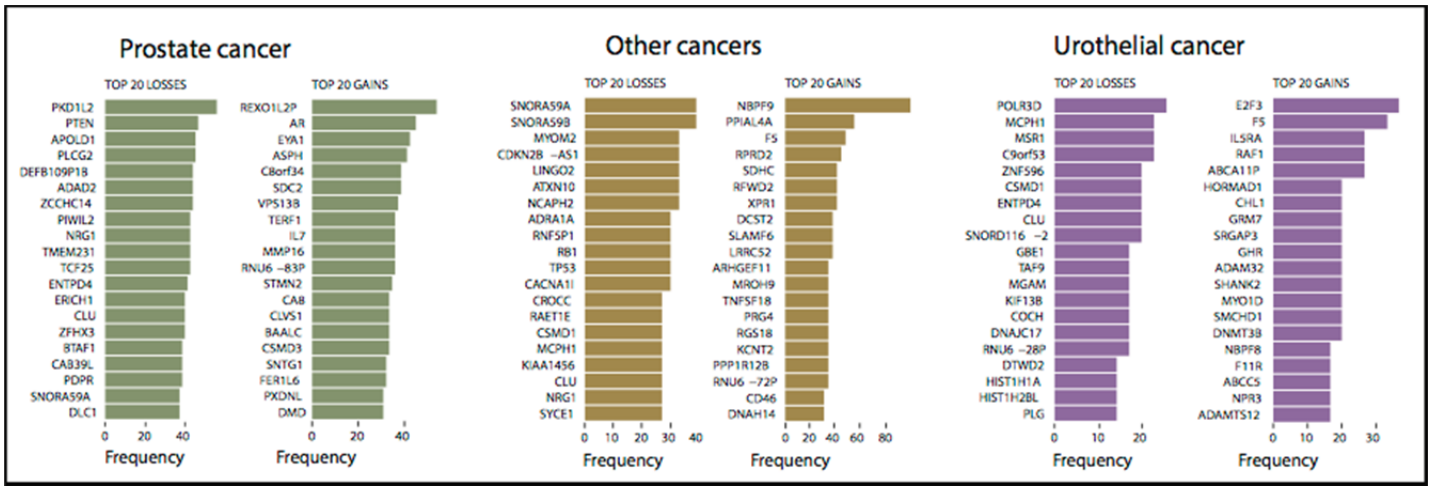

The ranking is performed at cytogenetic map location resolution by selecting for each location the most recurrent aberrant gene; if more genes demonstrate the same aberration frequency in a cytoband the gene with the lowest genomic position is selected as representative.

eFigure 7. Top 50 genes with focal and large scale copy number gains (A) and losses (B) across the cohort

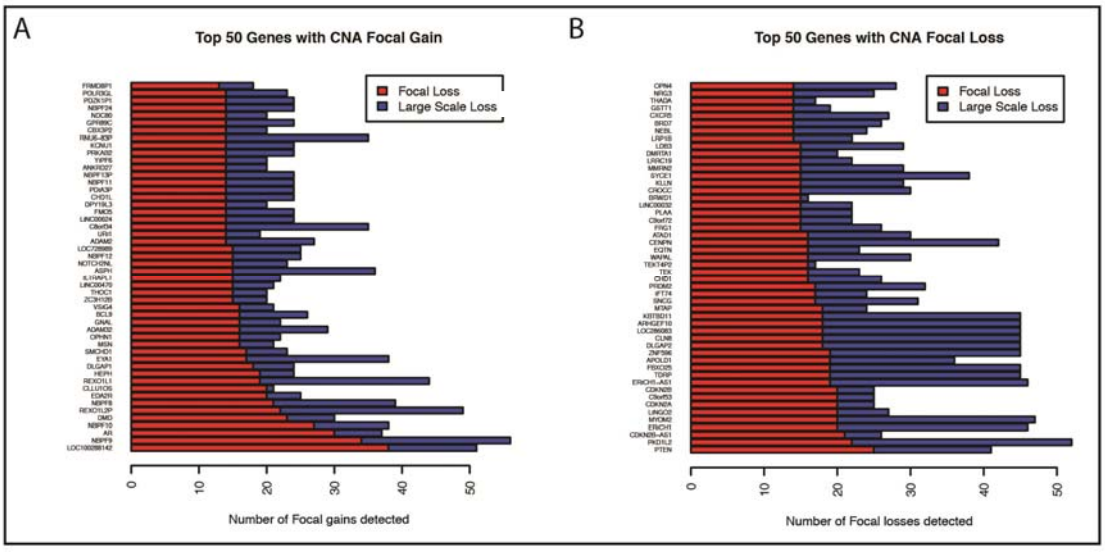

(A,B) are ordered by the number of focal gains and focal losses respectively. Notably AR was found in the top 50 genes with copy number gain and PTEN was found in the top 50 genes with copy number loss. AR copy number gain and PTEN copy number loss are hallmarks of prostate cancer. A significant proportion of prostate cancer samples make up our PM tumors.

eFigure 8. Summary of total number of copy number alterations across PM tumors

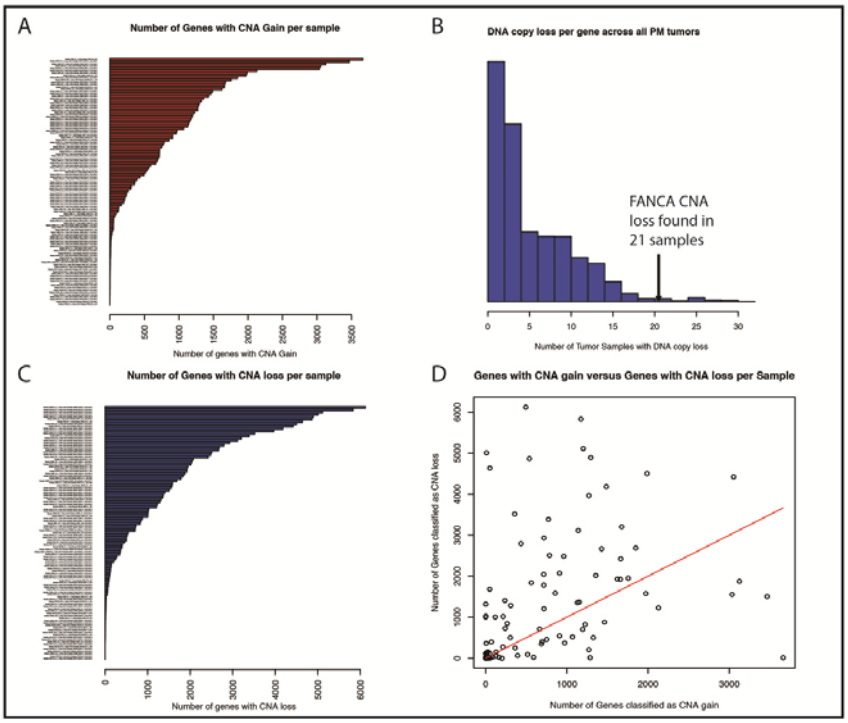

(A),(C),(D) illustrate the copy number alterations by gene across PM tumors. (A) shows the number of genes with copy number gain for each sample and (C) shows the number of genes with copy number loss for each sample. (D) is a comparison of the number of genes with copy number loss (y-axis) and the number of genes with copy number gain(x-axis). Each point in the plot represents the number of genes with copy number loss and the number of genes with copy number gain for a given PM tumor. The red line is the y=x line that serves as a comparison of whether we detect more genes with copy number loss or copy number gain. The data shown in (D) suggest that we do detect more genes with copy number loss for any given PM tumor. This observation is likely due to the fact that a large proportion of the PM tumors are prostate cancer. Large regions of copy number loss are often found in prostate cancer. (B) represents for any RefSeq gene, the number of samples where gene had a copy number loss detected. FANCA is highlighted on this figure. It is lost in 21 samples.

eFigure 9. An example of tumor evolution looking at serial biopsies from PM222, a patient with metastatic bladder carcinoma.

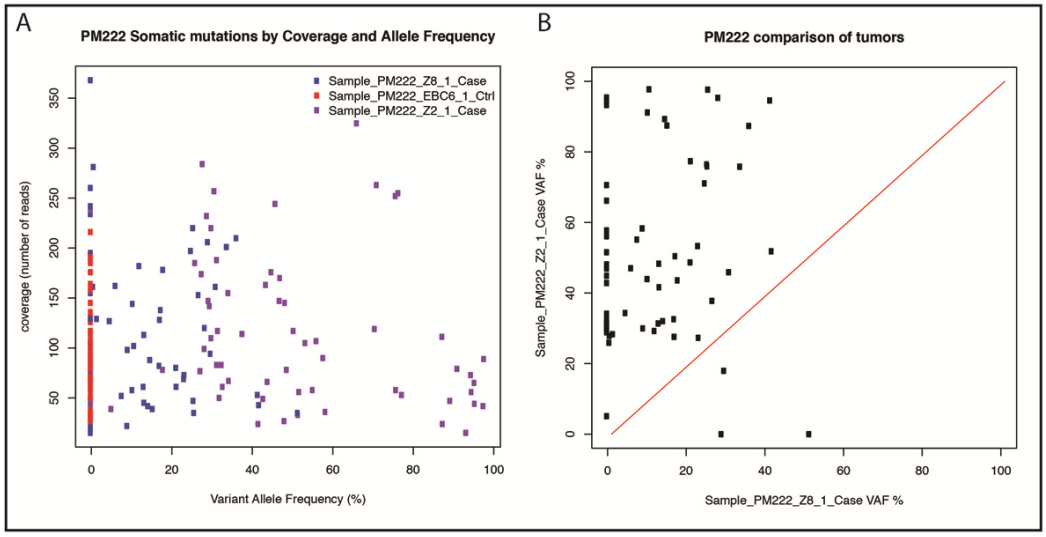

(A) somatic mutations are shown by coverage and allele frequency, (B) mutation correlation between patient matched pre-chemotherapy primary bladder tumor (X axis) and post-chemotherapy metastatic brain lesion (Y axis). (A) The coverage and allele frequency is plotted for the union of all somatic mutations detected in the primary (blue) and brain metastasis (purple). Samples that are similar should cluster near the same coverage and allele frequency. The control sample is shown in red as a negative control. (B) The allele frequencies for the union of all somatic mutations detected in the primary and brain metastasis are plotted. This is to reveal similarities and differences of the somatic mutation profile between the primary and metastasis. The red line represents the Y=X line and highlights the similarity of the primary and brain metastasis. Points that are in close proximity to the red line are mutations that have a similar allele frequency in both the primary and brain metastasis. Points that lay primarily on the x-axis or y-axis indicate somatic mutations unique to the primary or metastasis, respectively.

eFigure 10. PM12 somatic mutations by coverage and allele frequency (A) and (B) mutation correlation between primary (y- axis) and brain metastasis (x-axis)

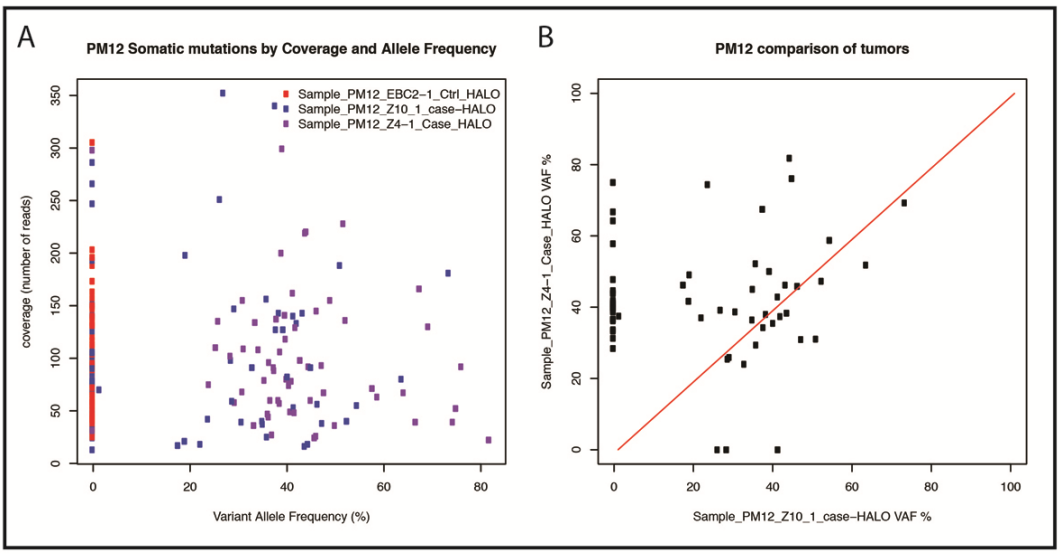

(A) The coverage and allele frequency is plotted for the union of all somatic mutations detected in the primary (blue) and brain metastasis (purple). Samples that are smilar should cluster near the same coverage and allele frequency. In A, the primary and brain metastasis cluster together, suggesting a similar somatic mutation profile. The control sample is shown in red as a negative control. (B) The allele frequencies for the union of all somatic mutations detected in the primary and brain metastasis are plotted. This is to reveal similarities and differences of the somatic mutation profile between the primary and brain metastasis. The red line represents the Y=X line and highlights the similarity of the primary and brain metastasis. Points that are in close proximity to the red line are mutations that have a similar allele frequency in both the primary and brain metastasis. Points that lay primarily on the y-axis or x-axis indicate somatic mutations unique to the primary or brain metastasis respectively.

eFigure 11. Point mutations across 5 metastatic sites of a 55 year old patient with metastatic prostate cancer at time of rapid autopsy

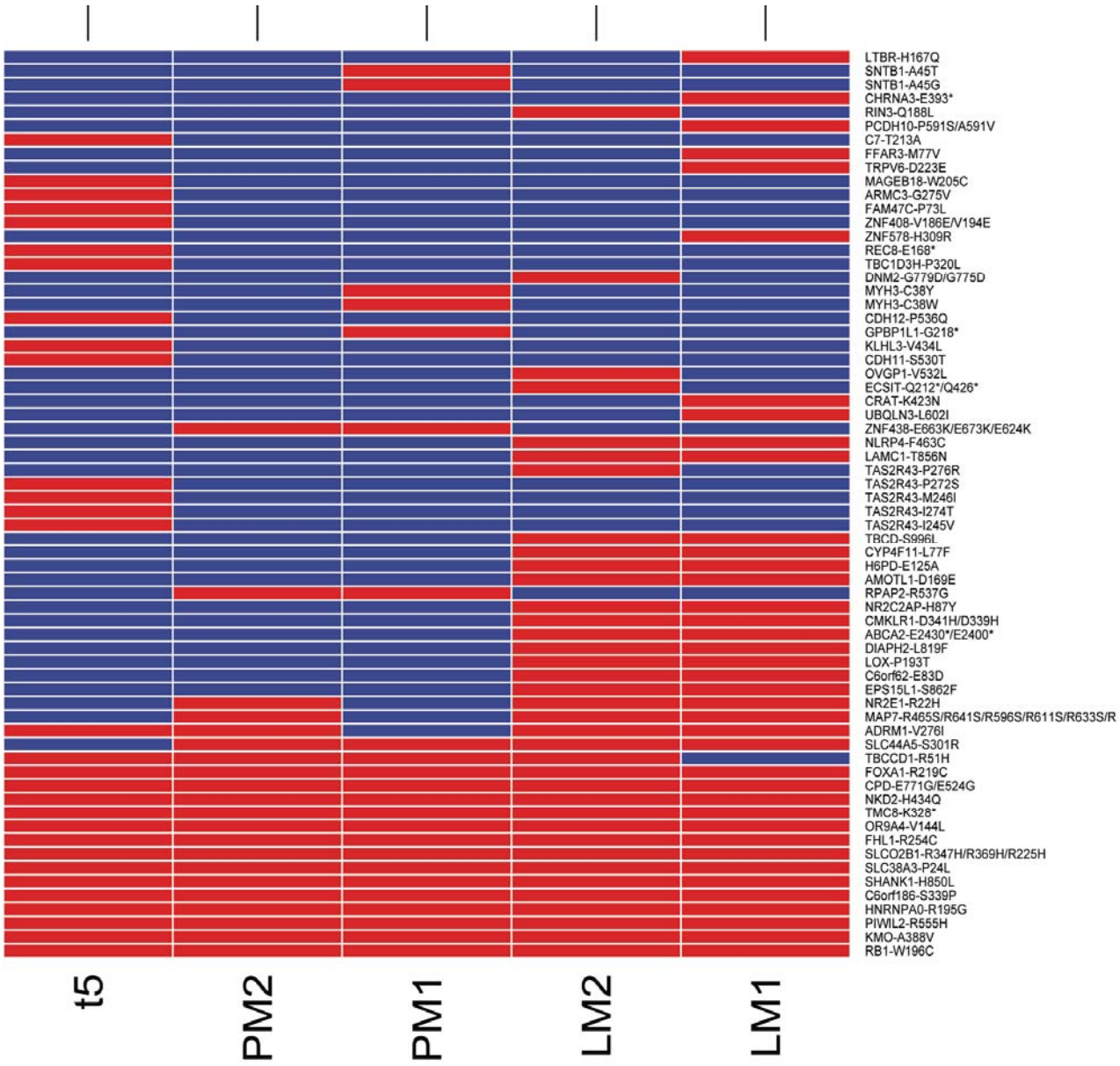

A total of 66 point mutations were identified across tumor sites, and a subgroup of mutations were shared across the different metastatic sites. This included a novel missense mutation (R219C) involving a known hot spot of FOXA1, a previously identified mutated gene in prostate cancer and a known cofactor involved in AR-signaling. Hemizygous deletion of PTEN was present in all metastatic sites. When tumors from different sites were compared, a cluster of point mutations specific for each site was also identified. Extensive somatic copy number alterations were present (data not shown), and there was an enrichment of structural variations and copy number alterations on chromosome 19, possibly suggesting a chromothripsis event. RED= mutation present, BLUE=no mutation. Sites included liver (LM1), liver (LM2), pelvic mass (PM1), pelvic lymph node (PM2), and right iliac lymph node (t5).

eFigure 12. CT scans from patient PM137, a patient with recurrent platinum refractory metastatic urothelial carcinoma. WES revealed ERBB2 (Her2) amplification, which was confirmed by immunohistochemistry and found to be 3+. The decision was made by referring physician to start PM157 on Her2 based therapy with herceptin and paclitaxel. She showed clinical improvement and scans after cycle 4 of Herceptin –based therapy showed stable pulmonary metastases and resolution or decreased size of her liver metastases (representative liver metastasis marked by arrows).

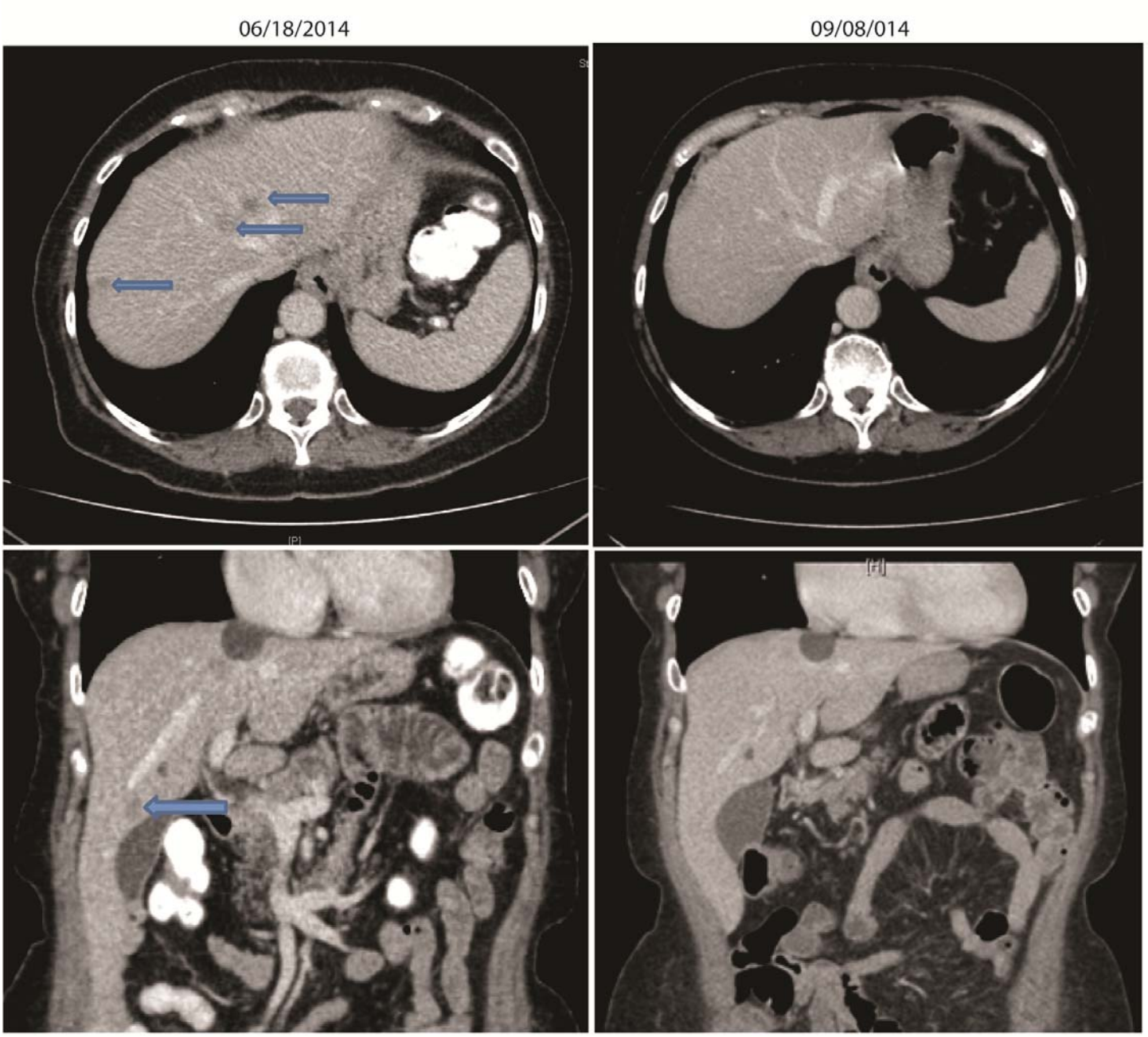

eFigure 13. Tracking tumor genomics between primary and metastatic samples from patient PM12

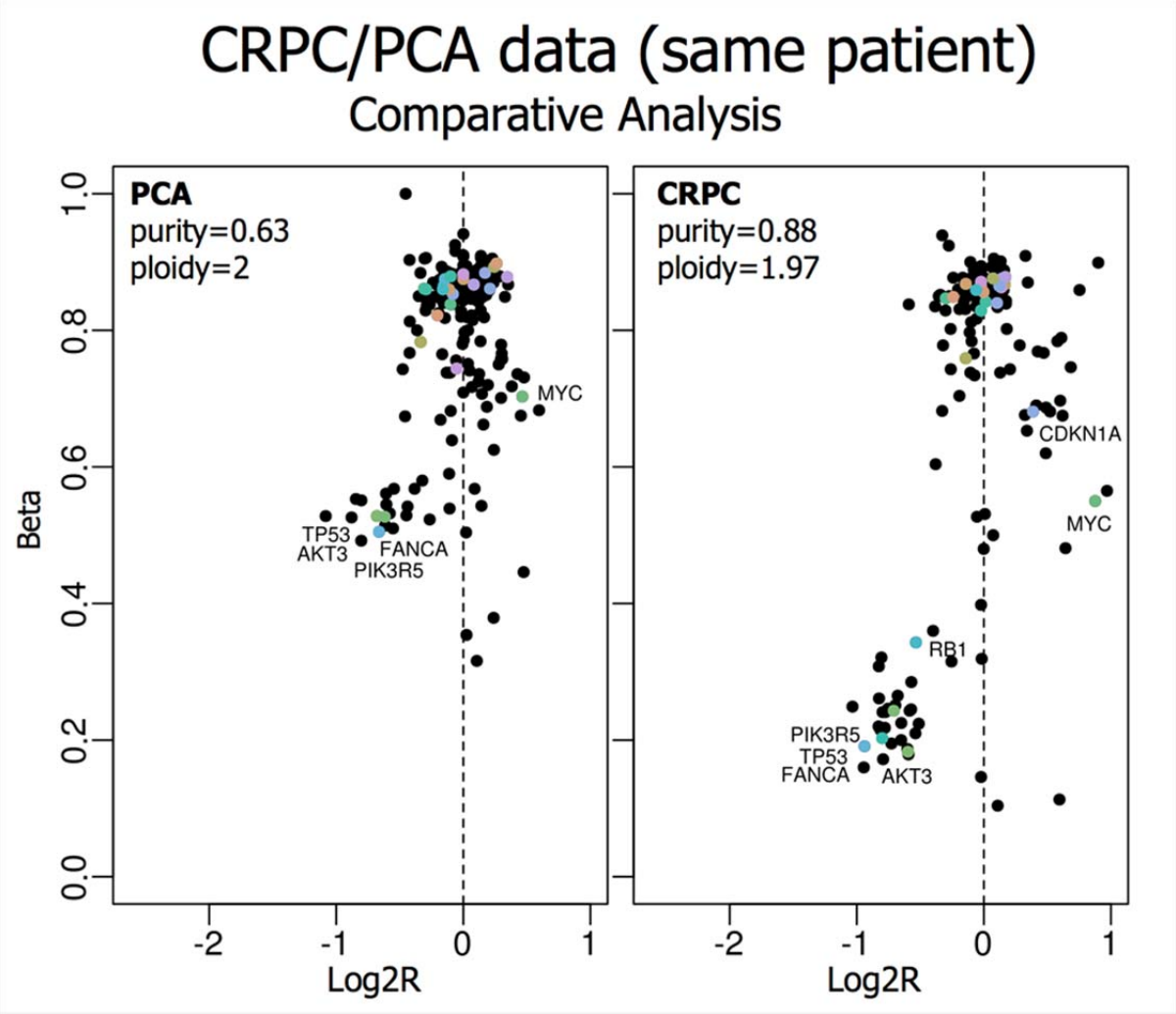

. CLONET analysis of patient PM12's primary tumor (PCA) **(A)** and his brain metastasis (CRPC) **(B)** demonstrating clonality of *FANCA* hemizygous deletion. For each genomic aberrant of his primary tumor (left) and brain metastasis (right), the plots show the percentage of neutral reads supporting the segment (reads that equally represent parental chromosomes, β) versus the corresponding copy number state (expressed as the $\log_2$ of the tumor to normal ratio R, Log R). DNA losses and gains have negative and positive values of $\log_2$ ratios. Colors indicate frequently mutated genes in PCA. The smaller the β, the more clonal the corresponding lesion. TP53, AKT3, FANCA, and PIK3R5 demonstrate consistent hemizygous deletion in both PCA and CRPC samples. Conversely, RB1 deletion emerges as subclonal hemizygous deletion in CRPC where copy number neutral state is observed in PCA.

eFigure 14. PM12 sequence data at *FANCA* gene showing hemizygous S1088F variant (Variant Allele Frequency or VAF 52%) in germline PM12 sample (control; bottom panel) and near-homozygous (VAF approximately 80%) in cases (PCA and CRPC), suggesting LOH at reference allele in tumor. At the mRNA level (top panels), FANCA mRNA is expressed but only the S1088F variant allele (100%).

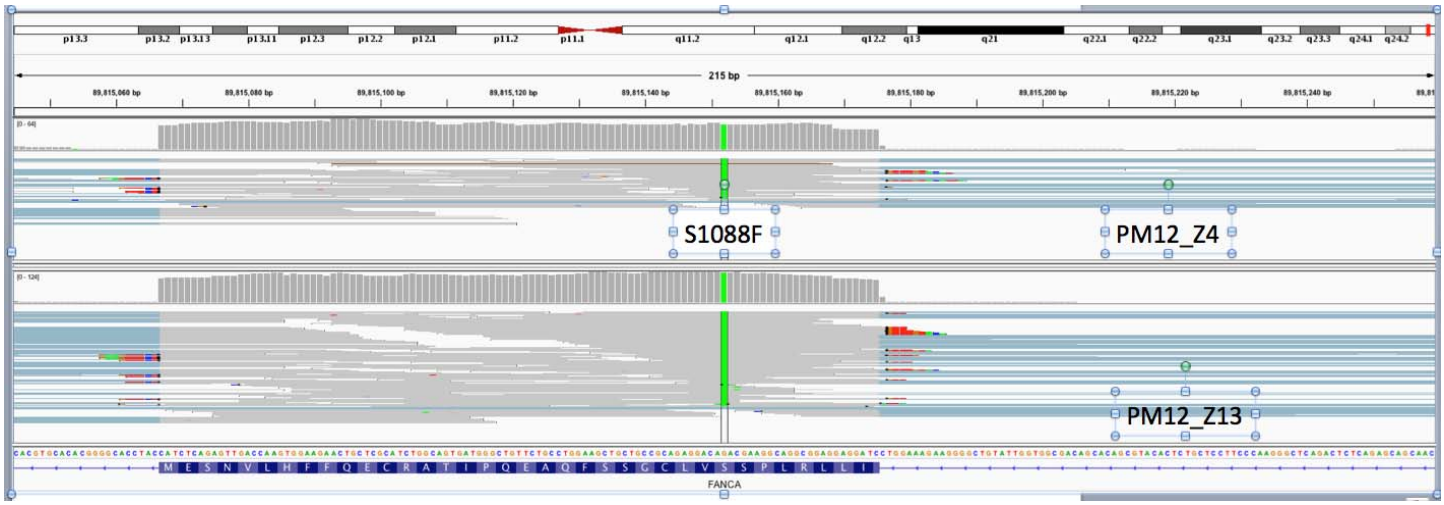

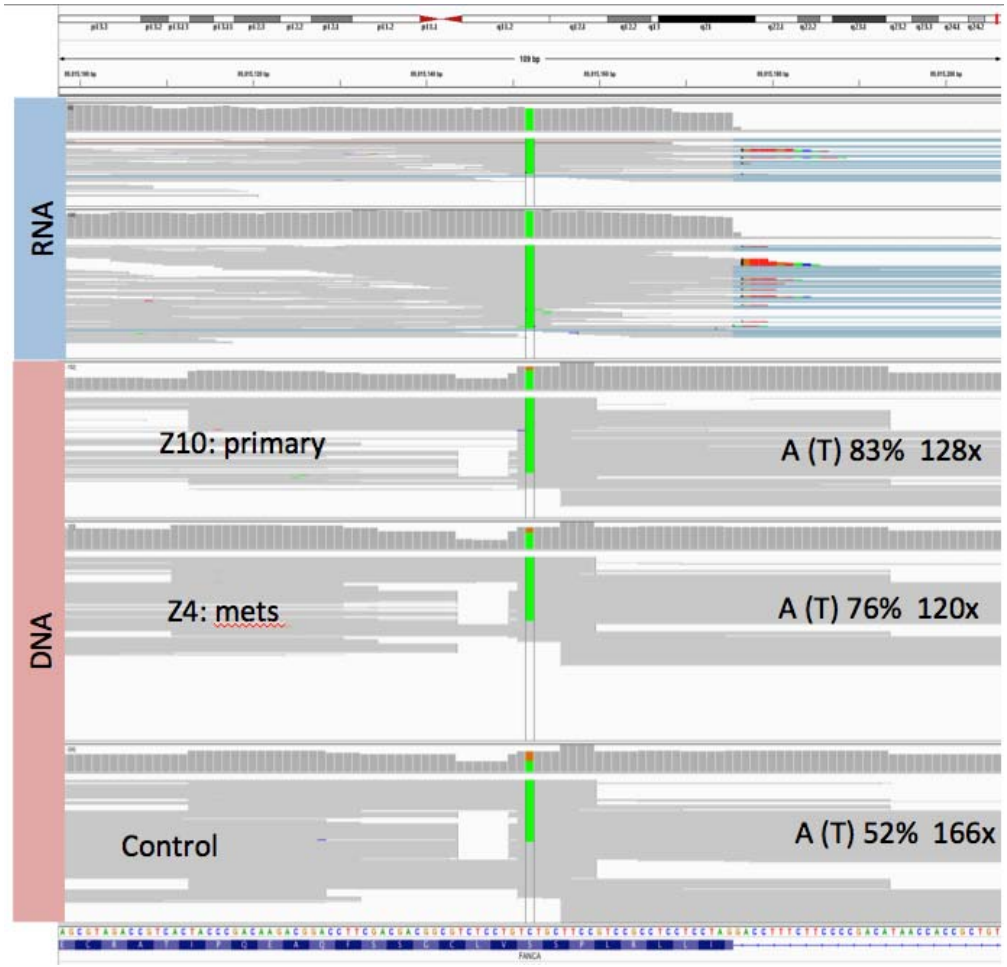

eFigure 15. FISH assay developed to assess *FANCA* deletion in prostate cancer

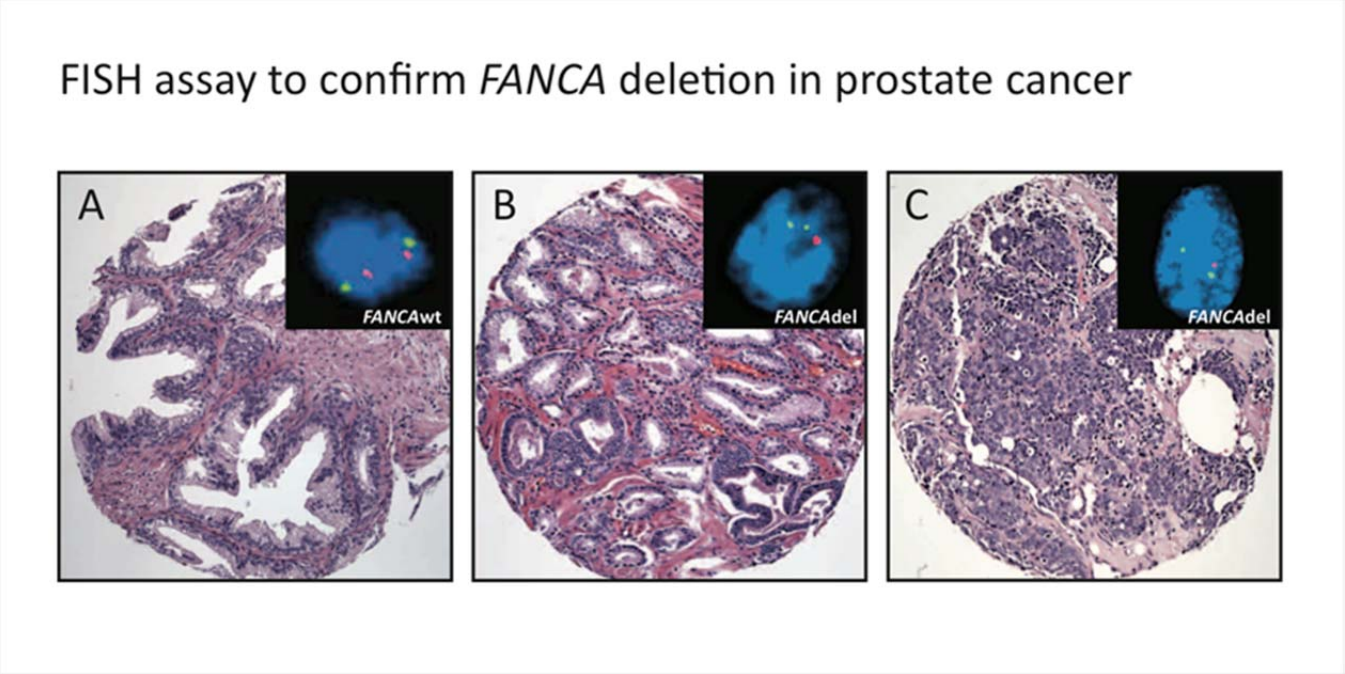

Dual color gene specific FISH assay (inset) demonstrates *FANCA* wild-type status in benign prostate tissue **(A).** In contrast, one of the alleles is deleted in a case of localized prostate cancer, Gleason grade 6 **(B),** and in one example of advanced castrate-resistant prostate cancer with neuroendocrine differentiation **(C).**

eFigure 16. In vitro data (A) Left: Isogenic fibroblasts with depletion of FANCA demonstrate enhanced platinum sensitivity compared to fibroblasts with stable over-expression of FANCA protein (IC50 2.48 uM vs. 6.11 uM, respectively), **Right:** Cisplatin dose response curves and IC50 values from independent isogenic FANCA negative fibroblasts with depletion of FANCA (no FANCA, IC50 0.3 uM) or these cells that stably over-express either the wild type FANCA cDNA (wt FANCA, IC50 1.8 uM) or the S1088F mutation cDNA (FANCA S1088F, IC50 0.8 uM) as shown in the Sanger Sequencing data belo , **(B)** Genome editing of *FANCA* in 22Rv1 cells by CRISPR results in increase in platinum sensitivity, **(C)** No significant changes in cellular proliferation are observed after genome editing of *FANCA* in 22Rv1 cells by CRISPR, (**D**) Cisplatin sensitivity in isogenic VCaP cells following control (siSCR) or siRNA knock-down of FANCA mRNA (siFANCA). Inset: Western blot of FANCA and GAPDH expression in VCaP cells following FANCA siRNA knockdown (Si-FANCA) or with scrambled control siRNA (siSc).

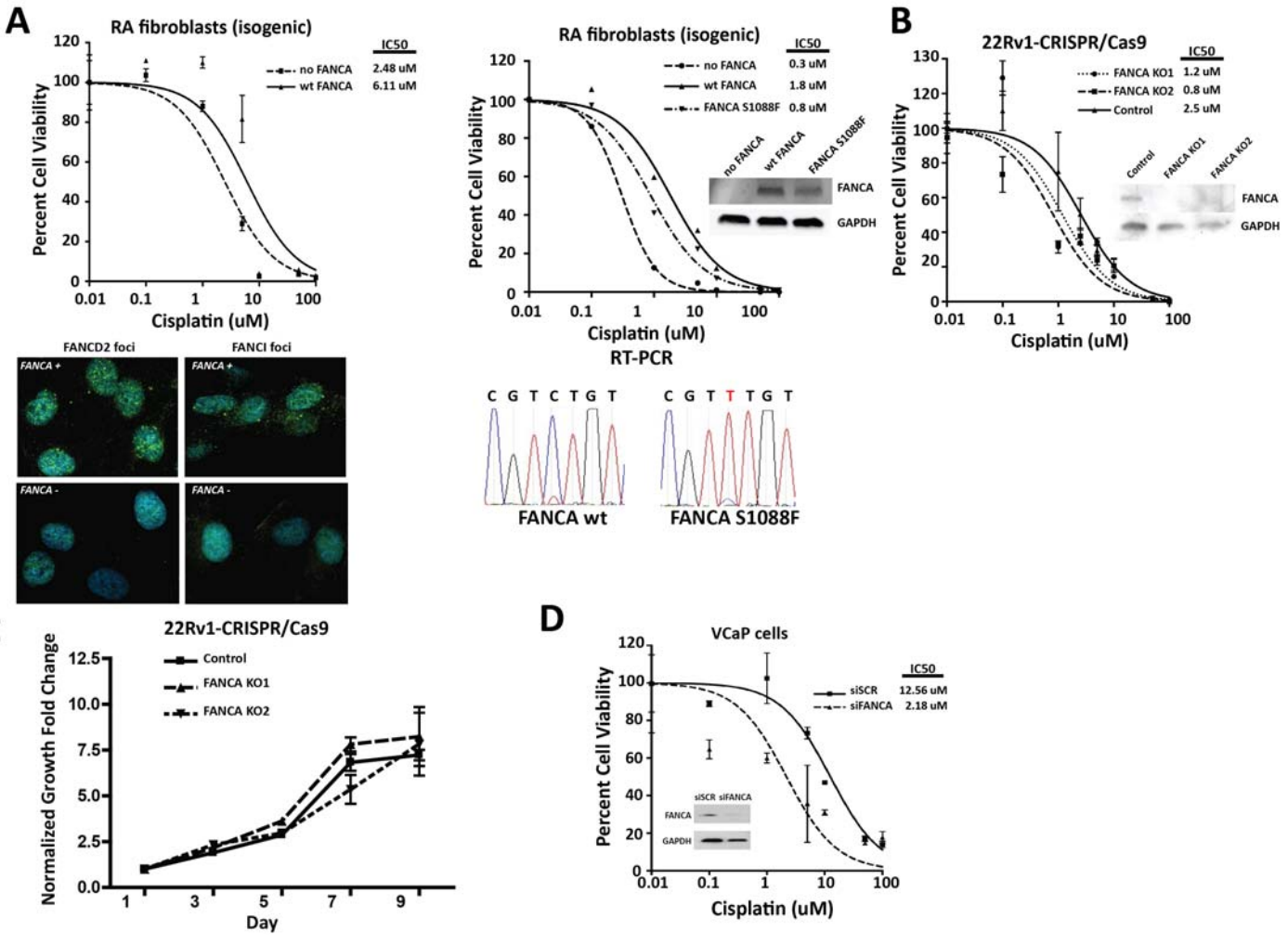

eFigure 17. H&E stained sections from of (A) the PM12-derived xenograft (LTL545) and (B) control NEPC tumor (LTL352), both of which showing NEPC histological features. Dual color gene specific FISH assay confirms FANCA copy number loss in LTL545 (Green= Centromeric Control Probes, Red = FANCA loci). Control xenograft (LTL352) is negative for *FANCA* deletion

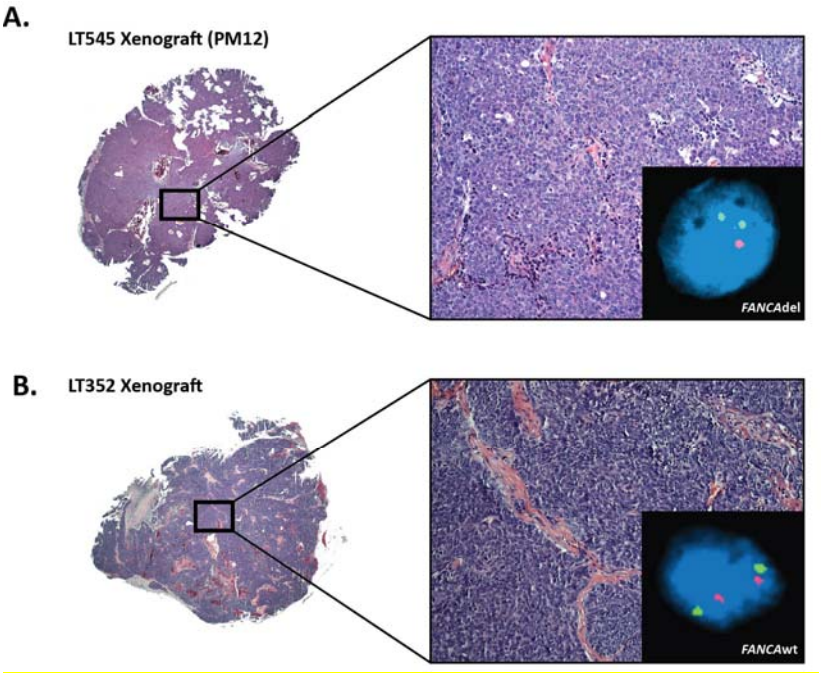

eFigure 18. Patient derived xenografts

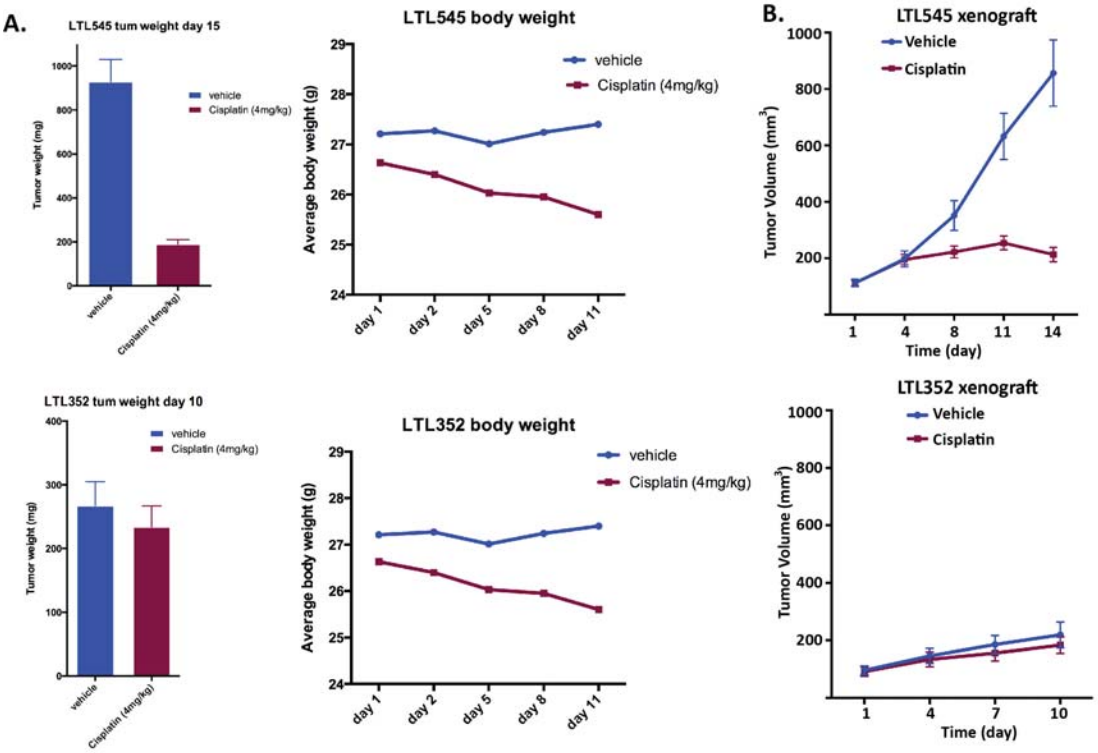

(A) Cisplatin treatment results in a significant decrease in tumor weight in in PDX of PM12 (LTL545) compared to control PDX (LTL352), without significant toxicity in either (body weight). **(B)** Average tumor size of the indicated xenograft before, during and after treatment with vehicle (blue lines) or Cisplatin (4mg/kg, day 1 and day 8, i.p. injection).

eFigure 19. Sanger cell line data across 590 cancer cell lines shows correlation between decreased FANCA gene expression across cell lines and cisplatin sensitivity as measured by IC50 values

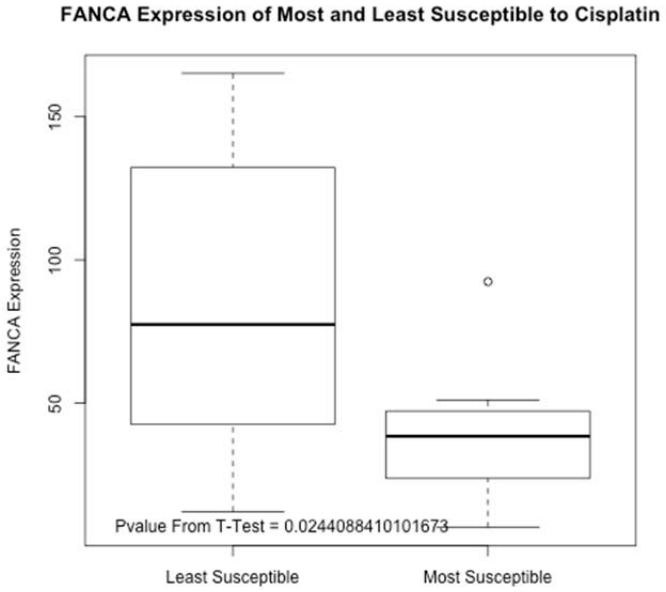

For gene expression analysis, RNA was hybridized to the HT-HGU133A Affymetrix whole genome array and normalized gene expression intensities were generated using the MAS5 algorithm (y axis= normalized mas5 gene expression intensities).

eFigure 20. Frequency of FANCA alterations across prostate cancer and other cancer cohorts (determined from TCGA data and other publically available datasets)

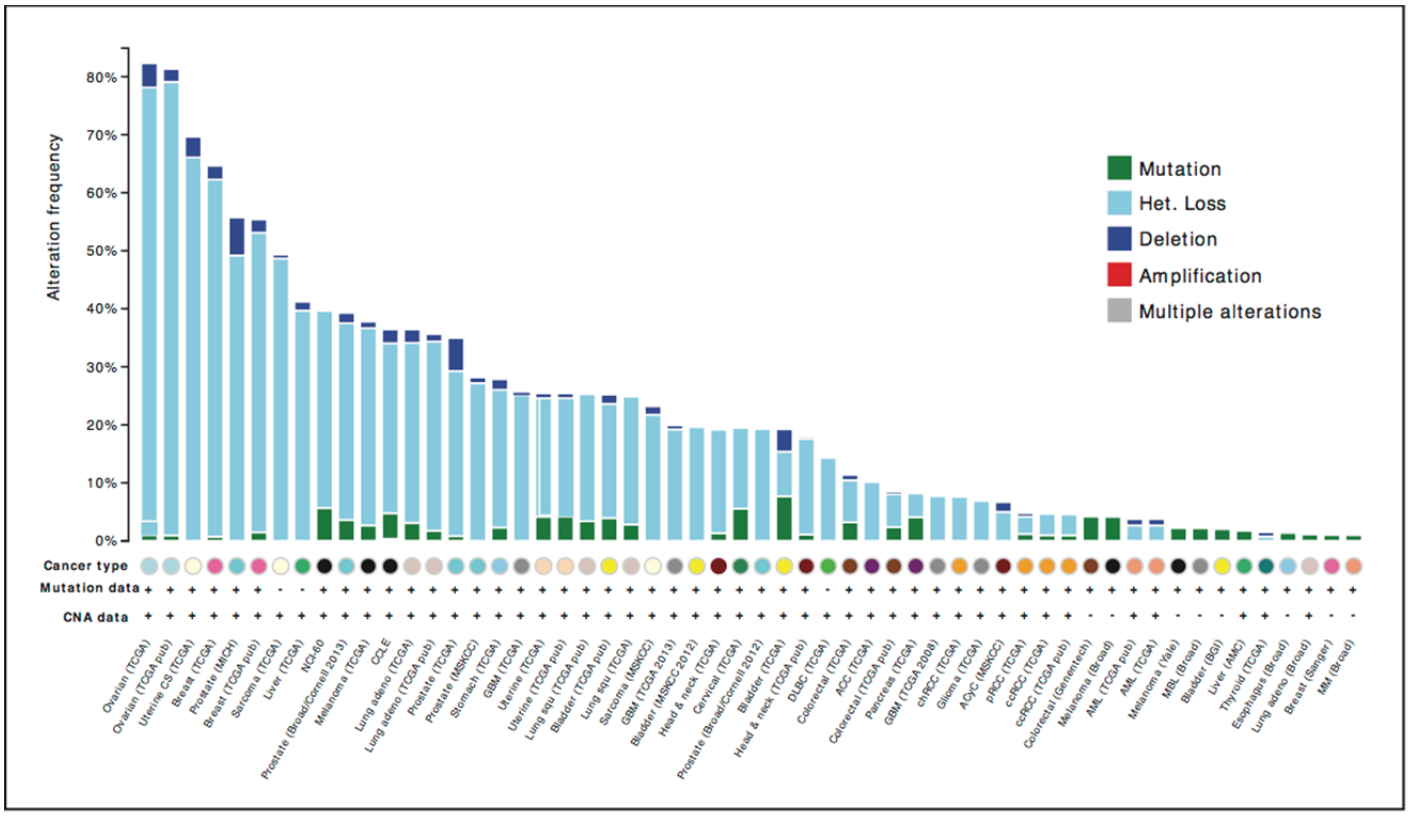

Supplementary Tables:

eTable 1. EXACT-1 Category 1 alterations (highlighted) and Category 2 alterations. Category 1 alterations are based on curating a subset of MyCancerGenome, Personalized Cancer Therapy, FDA pharmacogenomics list and recent literature). Category II alterations are 508 known cancer-associated genes according to the Sanger center Cancer Gene Census. All other somatic alterations of unknown clinical or biologic significance are annotated as Category III

ABL1	BRCA1	ERBB2	GNAQ	MAP2K2	ACSL3	ARHH	AXIN1	BCOR	BUB1B	CBFA2T1
ABL2	BRCA2	ERBB3	GNAS	MCL1	AF15Q14	ARID1A	BAP1	BCR	C12orf9	CBFA2T3
AKT1	CD79B	ERBB4	HRAS	MET	AF1Q	ARID2	BCL10	BHD	C15orf21	CBFB
AKT2	CDK4	FGFR1	IDH1	NRAS	AF3p21	ARNT	BCL11A	BIRC3	C15orf55	CBL
AKT3	CDK6	FGRF1	IDH2	PDGFRA	AF5q31	ASPSCR1	BCL11B	BLM	C16orf75	CBLB
ALK	CDKN2A	FGFR2	IKZF1	PIK3CA	AKAP9	ASXL1	BCL3	BMPR1A	C2orf44	CBLC
AR	CEBPA	FGFR3	JAK2	PTCH1	ALDH2	ATF1	BCL5	BRD3	CAMTA1	CCDC6
AURKA	CRKL	FGFR4	KIT	PTEN	ALO17	ATIC	BCL6	BRD4	CANT1	CCNB1IP1
BCL2	DNMT3A	FLT3	KRAS	SMO	APC	ATM	BCL7A	BRIP1	CARD11	CCND1
BRAF	EGFR	GNA11	MAP2K1	TSC1	ARHGEF12	ATRX	BCL9	BTG1	CARS	CCND2
CCND3	CDKN2C	CLTCL1	CRLF2	DDX6	ELKS	ERG	EZR	FANCG	FLJ27352	GAS7
CCNE1	CDX2	CMKOR1	CRTC3	DEK	ELL	ETV1	FACL6	FBXO11	FNBP1	GATA1
CD273	CEP1	CNOT3	CTNNB1	DICER1	ELN	ETV4	FAM22A	FBXW7	FOXL2	GATA2
CD274	CHCHD7	COL1A1	CYLD	DNM2	EML4	ETV5	FAM22B	FCGR2B	FOXO1A	GATA3
CD74	CHEK2	COPEB	D10S170	DUX4	EP300	ETV6	FAM46C	FEV	FOXO3A	GMPS
CD79A	CHIC2	COX6C	DAXX	EBF1	EPS15	EVI1	FANCA	FGFR1OP	FOXP1	GOLGA5
CDH1	CHN1	CREB1	DDB2	ECT2L	ERCC2	EWSR1	FANCC	FH	FSTL3	GOPC
CDH11	CIC	CREB3L1	DDIT3	EIF4A2	ERCC3	EXT1	FANCD2	FHIT	FUBP1	GPC3
CDK12	CIITA	CREB3L2	DDX10	ELF4	ERCC4	EXT2	FANCE	FIP1L1	FUS	GPHN
CDKN2a(p14)	CLTC	CREBBP	DDX5	ELK4	ERCC5	EZH2	FANCF	FLI1	FVT1	GRAF
H3F3A	HMGA1	HOXD13	IL7R	KDM5C	LCK	MADH4	MDS2	MLL3	MSF	MYCL1
HCMOGT-1	HMGA2	HRPT2	IRF4	KDM6A	LCP1	MAF	MECT1	MLLT1	MSH2	MYCN
HEAB	HNRNPA2B1	HSPCA	IRTA1	KDR	LCX	MAFB	MED12	MLLT10	MSH6	MYD88
HERPUD1	HOOK3	HSPCB	ITK	KIAA1549	LHFP	MALT1	MEN1	MLLT2	MSI2	MYH11
HEY1	HOXA11	IGH@	JAK1	KIF5B	LIFR	MAML2	MITF	MLLT3	MSN	MYH9
HIP1	HOXA13	IGK@	JAK3	KLF4	LMO1	MAP2K4	MKL1	MLLT4	MTCP1	MYST4
HIST1H3B	HOXA9	IGL@	JAZF1	KLK2	LMO2	MAX	MLF1	MLLT6	MUC1	NACA
HIST1H4I	HOXC11	IL2	JUN	KTN1	LPP	MDM2	MLH1	MLLT7	MUTYH	NBS1
HLF	HOXC13	IL21R	KCNJ5	LAF4	LRIG3	MDM4	MLL	MN1	MYB	NCOA1
HLXB9	HOXD11	IL6ST	KDM5A	LASP1	LYL1	MDS1	MLL2	MPL	MYC	NCOA2
NCOA4	NOTCH1	NUP98	PBRM1	PICALM	POU2AF1	PSIP2	RARA	RPL5	SDHD	SIL
NDRG1	NOTCH2	OLIG2	PBX1	PIK3R1	POU5F1	PTCH	RB1	RPN1	SEPT6	SLC34A2
NF1	NPM1	OMD	PCM1	PIM1	PPARG	PTPN11	RBM15	RUNDC2A	SET	SLC45A3
NF2	NR4A3	P2RY8	PCSK7	PLAG1	PPP2R1A	RAB5EP	RECQL4	RUNX1	SETBP1	SMARCA4
NFE2L2	NSD1	PAFAH1B2	PDE4DIP	PML	PRCC	RAC1	REL	RUNXBP2	SETD2	SMARCB1
NFIB	NT5C2	PALB2	PDGFB	PMS1	PRDM1	RAD51L1	RET	SBDS	SF3B1	SMARCE1
NFKB2	NTRK1	PAX3	PDGFRB	PMS2	PRDM16	RAF1	RNF43	SDC4	SFPQ	SOCS1
NIN	NTRK3	PAX5	PER1	PMX1	PRF1	RALGDS	ROS1	SDH5	SFRS3	SOX2
NKX2-1	NUMA1	PAX7	PHF6	PNUTL1	PRKAR1A	RANBP17	RPL10	SDHB	SH2B3	SRGAP3
NONO	NUP214	PAX8	PHOX2B	POT1	PRO1073	RAP1GDS1	RPL22	SDHC	SH3GL1	SRSF2
SS18	SUZ12	TCL1A	TIF1	TPM3	TSC2	WIF1	ZNF198			
SS18L1	SYK	TCL6	TLX1	TPM4	TSHR	WRN	ZNF278			
SSH3BP1	TAF15	TERT	TLX3	TPR	TTL	WT1	ZNF331			
SSX1	TAL1	TET2	TMPRSS2	TRA@	U2AF1	WTX	ZNF384			
SSX2	TAL2	TFE3	TNFAIP3	TRAF7	USP6	WWTR1	ZNF521			
SSX4	TCEA1	TFEB	TNFRSF14	TRB@	VHL	XPA	ZNF9			
STAT3	TCF1	TFG	TNFRSF17	TRD@	VTI1A	XPC	ZRSR2			
STK11	TCF12	TFPT	TNFRSF6	TRIM27	WAS	XPO1				
STL	TCF3	TFRC	TOP1	TRIM33	WHSC1	YWHAE				
SUFU	TCF7L2	THRAP3	TP53	TRIP11	WHSC1L1	ZNF145				

eTable 2. Five rapid autopsy cases

Primary tumor	Prostate	Prostate	Bladder	Cerebellum	Prostate
Time from Diagnosis to Death	18 months	3 years	20 months	5 years, 4mo	22 months
Prior systemic therapies	leuprolide acetate, cisplatin-etoposide	leuprolide acetate; bicalutamide; docetaxel/prednisone; abiraterone/prednisone	gemcitabine+cispatin; docetaxel+ramicirumab (on trial)	Metronomic therapy (thalidomide, fenofibrate, celecoxib, cyclophosphamide, etposide); sunitinib; lapatinib-bevacizumab (on trial); oral etoposide; 5FU on St Jude protocol; gemcitabine; perifosine; BKM120	leuprolide acetate; docetaxel/prednisone; abiraterone/prednisone
Metastatic sites	Liver, lymph nodes	Liver, adrenal gland, bone, lymph nodes	Liver, lymph nodes	Central nervous system including spinal cord	Brain, lung, liver, adrenal gland, testes, bone, lymph nodes
Pathology	Small cell carcinoma	Poorly differentiated adenocarcinoma	Papillary urothelial carcinoma	Anaplastic ependymoma	Poorly differentiated adenocarcinoma
# of sites sequenced	6	5	8	3	6
DNA conc. (ng/ul)(avg)	283	43	109	87	67
Average Coverage (range)	302.9x (281-328)	85.3x (83-87)	87.4x (75-99)	78x (67-84)	84.4x (80-88)
Average capture efficiency (% range)	71.90 (71.28-72.57)	86.39 (85.69-87.18)	85.59 (82.84-90.04	86.76 (86.37-86.96)	84.88 (84.36-85.44)

eTable 3. Crest variants comparison by WGS. Number of predicted SVs per tumor sample, broken up by type of variant (DEL – deletions, INV – inversions, CTX – interchromosomal translocations, ITX – intrachromsoml translocations, INS – insertions). PM12 samples have the highest number of predicted SVs, predominantly deletions. PM0 samples have strikingly high numbers of intrachromosomal translocations, most of which affect chr19. PM1 is the quietest sample in the cohort with only few predicted SVs.

Structural variants called by Crest	DEL	INV	CTX	ITX	INS
PM0_Tissue LM1_A	86	2	56	125	66
PM0_Tissue LM2_A	68	2	58	128	65
PM1_Tissue	1	0	5	6	0
PM4_Tissue	110	2	26	18	26
PM7_Tissue	36	1	18	23	15
PM12_Tissue Z4_2	254	0	63	44	13
PM12_Tissue Z13_1	261	1	66	44	9

eTable 4. **FANCI and FANCD2 foci formation data.** Fisher's exact test p values are shown for the number of foci forming cells in the presence or absence of 1 uM MMC for 24 hours.

RA fibroblasts

No DNA damage

		FANCA protein	
		pos	neg
FANCI foci	pos	83	15
	neg	323	393
	Total # of cells	406	408
	Fisher's exact test, two-tailed p < 0.0001		

		FANCA protein	
		pos	neg
FANCD2 foci	pos	17	0
	neg	386	200
	Total # of cells	403	200
	Fisher's exact test, two-tailed p= 0.0012		

DNA damage

		FANCA protein	
		pos	neg
FANCI foci	pos	89	19
	neg	331	385
	Total # of cells	420	404
	Fisher's exact test, two-tailed p < 0.0001		

		FANCA protein	
		pos	neg
FANCD2 foci	pos	83	15
	neg	323	393
	Total # of cells	406	408
	Fisher's exact test, two-tailed p < 0.0001		

22Rv1 cells

No DNA damage

		FANCA protein	
		pos	neg (KO1)
FANCI foci	pos	177	51
	neg	228	360
	Total # of cells	405	411
	Fisher's exact test, two-tailed p < 0.0001		

		FANCA protein	
		pos	neg (KO1)
FANCD2 foci	pos	250	70
	neg	155	190
	Total # of cells	405	260
	Fisher's exact test, two-tailed p < 0.0001		

		FANCA protein	
		pos	neg (KO2)
FANCI foci	pos	177	6
	neg	228	135
	Total # of cells	405	141*
	Fisher's exact test, two-tailed p < 0.0001		

		FANCA protein	
		pos	neg (KO2)
FANCD2 foci	pos	250	87
	neg	155	317
	Total # of cells	405	404
	Fisher's exact test, two-tailed p < 0.0001		

DNA damage							
		FANCA protein				FANCA protein	
		pos	neg (KO1)			pos	neg (KO1)
FANCI foci	pos	144	24	FANCD2 foci	pos	107	14
	neg	64	148		neg	100	190
	Total # of cells	208	172*		Total # of cells	207	204
	Fisher's exact test, two-tailed p < 0.0001				**Fisher's exact test, two-tailed p < 0.0001**		
		FANCA protein				FANCA protein	
		pos	neg (KO2)			pos	neg (KO2)
FANCI foci	pos	144	40	FANCD2 foci	pos	107	26
	neg	64	157		neg	100	176
	Total # of cells	208	197*		Total # of cells	207	202
	Fisher's exact test, two-tailed p < 0.0001				**Fisher's exact test, two-tailed p < 0.0001**		
* low number of cells (i.e. < 200 nuclei evaluable)							

eTable 5. **FANCI and FANCD2 foci formation percentages** based on the numbers shown in eTable 4.

RA fibroblasts

		FANCI foci	% cells with foci formation
No DNA damage	FANCA protein	pos	20
		neg	4
DNA damage	FANCA protein	pos	21
		neg	5

		FANCD2 foci	% cells with foci formation
No DNA damage	FANCA protein	pos	4
		neg	0
DNA damage	FANCA protein	pos	87
		neg	37

22Rv1 cells

		FANCI foci	% cells with foci formation
No DNA damage	FANCA protein	pos	44
		neg (KO1)	12
		neg (KO2)	4
DNA damage	FANCA protein	pos	69
		neg (KO1)	14
		neg (KO2)	20

		FANCD2 foci	% cells with foci formation
No DNA damage	FANCA protein	pos	62
		neg (KO1)	27
		neg (KO2)	22
DNA damage	FANCA protein	pos	52
		neg (KO1)	7
		neg (KO2)	13

eTable 6. **Table summarizing tumor sizes and weight of PDXs** at the indicated day. P values are obtained using mixed effect analysis.

Patient derived xenograft LTL352					
Mean Tumor volume (mm^3)	**day 1**	**day 4**	**day 7**	**day 10**	
Control	95.5331	145.5715733	185.1904167	219.3082667	
Cisplatin	90.976	133.32876	155.82584	183.4894	
SD					
Control	54.71264193	91.09554903	109.9639587	155.8522821	
Cisplatin	59.57827007	91.93867824	100.9638558	103.285444	
SE					
Control	15.79417927	26.29701988	31.74386056	44.99067852	
Cisplatin	16.52403905	25.49920143	28.0023353	28.64622803	
Mixed effect analysis	**p = 0.0615**				
Tumor weight (mg) at day 11					
	Control	Cisplatin			
mean	267.5	233.8461538			
SD	129.1317157	118.9914886			
SE	37.27711541	33.00230104			
Wilcoxon Rank-sum test	**p= 0.7266**				
Mouse body weight (g)	day 1	day 2	day 5	day 8	day 11
Control	27.21428571	27.27142857	27.01428571	27.24285714	27.4
Cisplatin	26.625	26.4	26.025	25.95	25.6
Body weight loss (%)					
		-		-	-
Control	0	0.209973753	0.734908136	0.104986877	0.682414698
Cisplatin	0	0.845070423	2.253521127	2.535211268	3.849765258
Patient derived xenograft LTL545					
Mean Tumor volume (mm^3)	**day 0**	**day 4**	**day 8**	**day 11**	**day 14**
Control	107.6000907	184.5862552	302.5717961	556.6603486	737.8032659
Cisplatin	103.2369253	193.3369474	195.3237928	211.4865191	196.4434782
SD					
Control	51.67602449	108.588311	205.8890067	321.5034824	473.2381915
Cisplatin	47.35739357	67.9632976	93.19247781	113.6447641	103.7670934
SE					
Control	12.91900612	26.33653387	47.23417757	73.75795736	108.568287
Cisplatin	11.48585505	16.9908244	21.37982069	25.41174179	25.16721686
Mixed effect analysis	**p = 0.0001**				

Tumor weight (mg) at day 15					
	Control	Cisplatin			
mean	926.6666667	193.3333333			
SD	395.4503159	86.32717389			
SE	102.1048325	22.28958045			
Wilcoxon Rank-sum test	**p < 0.0001**				
Mouse body weight (g)	day 1	day 2	day 5	day 8	day 11
Control	27.21428571	27.27142857	27.01428571	27.24285714	27.4
Cisplatin	26.625	26.4	26.025	25.95	25.6
Body weight loss (%)	day 1	day 2	day 5	day 8	day 11
		-		-	-
Control	0	0.209973753	0.734908136	0.104986877	0.682414698
Cisplatin	0	0.845070423	2.253521127	2.535211268	3.849765258

eAppendix. Bioinformatics and Statistical Considerations for Supplementary Figures and Tables

All analyses were performed based on data generated by IPM-Exome-pipeline v0.9 or otherwise mentioned in legend. The IPM-Exome-pipeline v0.9 is described in the Supplementary Methods section. Plotting and statistical testing was performed using the R statistical software (version 3.0.2), Prism or Graphpad as indicated.

In **eFigure 2**, the boxplot was drawn using R with default parameters (boxplot function). Tumor purities are obtained from running the CLONET program with default parameters as described in Supplementary Methods. A t-test was used to calculate the p-value (t.test function).

In **eFigure 3,** the X-Y plot was drawn using R (plot function). A spearman correlation and associated test (cor.test function in R) was used to calculate the correlation between X and Y axes. The abline function in R was used to draw the X=Y line.

In **eFigure 4**, boxplots are created using the boxplot function in R. Number of mutations, CNA gains, CNA losses, average coverage, indels are all obtained from running IPM-Exome-pipeline v0.9 on sequence data from 154 tumor-normal pairs from 97 advanced cancer patients as discussed in the main text. Boxplot show median values, upper and lower quartiles as well as samples that are located outside 1.5 times the interquartile range above the upper quartile and bellow the lower quartile. Samples are divided into two groups, FFPE and fresh-frozen.

In **eFigure 7,** we plotted the number of times genes are found within regions of focal loss, large-scale loss, focal gain, large-scale gain. In this analysis, gene annotation was obtained from RefSeq downloaded in June 2014 from UCSC Genome Browser (Downloads section). The annotated copy number events are obtained from IPM-Exome-pipeline v0.9 and reformatted to draw these plots. In IPM-Exome-pipeline v0.9, a focal event is defined as containing 50 genes or less. The plots are drawn using the barplot function in R and ordered by focal event frequency.

In **eFigure 8,** we used the barplot function in R to plot the number of genes with CNA gains for each sample, according to IPM-Exome-pipeline v0.9 (Fig S5A). This analysis includes both focal and large-scale events. In S5B, the distribution of times each gene was found to be deleted in our cohort. FANCA was deleted in 21 samples. Fig S5C is the same as S5A but for losses and was also drawn using the barplot function in R. Samples are ordered by number of events. Fig S5D plots number of gene losses vs number of gene gains for all samples using the plot function in R, with abline function used to plot the Y=X line.

In **eFigure 9,** we plot variant allele frequency (VAF; the number of reads supporting each mutation divided by the coverage at that mutation) versus coverage using the plot function in R. VAFs were obtained by running IPM-Exome-pipeline v0.9 on the PM222 samples. All mutations analyzed are somatic mutations and accordingly their VAF is 0 in the control sample. In Figure S6A, we show VAF allele frequencies for the union of all somatic mutations detected in the primary and brain metastasis by running IPM-Exome-pipeline v0.9. The plot R function was used to make this plot. The red line (Y=X) was plotted using the abline function in R.

In **eFigure 13,** we used the CLONET software as part of IPM-Exome-pipeline v0.9 to generate Log R and β values for each CNA segments, then annotated segments with key genes. Plots show percentage of neutral reads supporting the segment (reads that equally represent parental chromosomes, β) versus the corresponding copy number state (expressed as the $\log_2$ of the tumor to normal ratio R, Log R) and were made the plot function in R. DNA losses and gains have negative and positive values of $\log_2$ ratios. The smaller the β, the more clonal the corresponding lesion. The CLONET software was also used to generate ploidy and purity estimates from the sequencing data.

In **eFigure 14,** we used the Integrated Genome Viewer software to show reads at the location of the S1088F variant in FANCA. For this analysis, we loaded the IPM-Exome-pipeline v0.9 BAM files (as well as RNAseq BAM files) into IGV. VAFs shown in this plot are the ones shown in IGV.

In **eFigure 19,** we draw a boxplot of FANCA expression for low vs high GI50 cell lines for cisplatin according to the Sanger cell line data. FANCA expression was compared using the t.test function in R.

In **eTable 3,** we show the number of events called by CREST, including DEL – deletions, INV – inversions, CTX – interchromosomal translocations, ITX – intrachromosomal translocations, INS – insertions. CREST is a tool for structural variation calling that was used with default parameters for these analyses(9).

Precision Medicine Program at WCMC

STANDARD OPERATING PROCEDURES (SOP)

PRECISION MEDICINE (PM) TISSUE PROCESSING

Table of content

A. Introduction

Purpose

This manual of procedures (MOP) is to standardize the method for collecting and handling biospecimens collected from participants in the "Precision Medicine" program. The biospecimens include needle biopsies of tumors, bone marrow biopsies, excisional biopsies of tumors for the extraction of DNA and RNA.

It is critical that all samples have to be collected, processed and stored in a uniform and consistent manner. Deviations from these procedures should be annotated in the meta-data that accompanies the samples.

Scope

These procedures apply to all personnel involved in the collection and handling of tumor biopsies.

Precaution

Universal precautions for handling potentially infectious biospecimens should be followed at all times (e.g. gloves; safety needles; etc). All acquisition materials should be disposed of in appropriate biohazard containers.

B. Material and Equipment required

MATERIAL	NUMBER/AMT	VENDOR	CAT #
Tissue Tek™ standard-size cryomolds	1 to 5 per sample	Fisher	NC9511236
Tissue Tek™ OCT	1 BOTTLE	Fisher	14-373-65
Cork Disk 22mm	1 per crymold		
Insulated NalGene Container	1		
Dry ice	1 container		
Wet ice	1 container		
Methylbutane	As needed		
100% Alcohol - 200 Proof Pure Ethanol	As needed		
95% Alcohol – 190 Proof Pure Ethanol			
Blue Pads and Markers	As needed	Fisher	507105 NC9319816
1.7 ml Posi-Click tube (Denville)	8	Fisher	C2170
Gloves (non-sterile)	1 box		
Ruler	1		
Camera	1		
Superfrost plus slides	10 slides		
Scalpel	3		
Tweezers	1		
Microscope	1		
Hematoxylin			
Eosin			
Bluing Reagent			
Large container for water			
Xylene			
Manual Hand Staining Unit			
Thermo Scientific Cytoseal- XYL			
Microscope Cover Glass 24x50mm			
-21 Cryostat	1		

Large Forceps - 12”	1		
Paper towel			
Insulated NalGene Container	1		
Small Zip lock bag - 3x6	1 per case		
Metal Chucks	1 per block		
Leica Slide Etcher			
24 Count Slide Rack	1		
Spec-Tec Resistant Disposable Cut Gloves	1		
Small Pencil Thin Brush	1		
High-profile disposable Blades #818 (10x50)	1		
Biohazard Sharps Disposal Container	1		
-80°C Freezer	1		

C. Preparing for tissue collection

1. Contact info

- Contact all the team members once the date of the procedure is known. A good communication between the research staff and the surgery team is required to ensure that the sample is collected according to the SOP.

- Research team

Mark A. Rubin, Pathology
rubinma@med.cornell.edu

Himisha Beltran, Oncology
hip9004@med.cornell.edu

Marc Schiffman, Interventional Radiology
mas9252@med.cornell.edu

Juan Miguel Mosquera, Pathology
jmm9018@med.cornell.edu

Brian Robinson, Pathology
brr2006@med.cornell.edu

Myriam Kossai, Pathology
myk2003@med.cornell.edu

Jacqueline Fontugne, Pathology

jaf2034@med.cornell.edu

Rob Kim, Program Manager
rok2011@med.cornell.edu

Jessica Padilla, Technician
jep2023@med.cornell.edu

Latasha McNeil, Technician
lam9035@med.cornell.edu

Leticia Dizon, Technician
led9016@med.cornell.edu

2. Preparation and PM specimen Worksheet

- Arrive at the collection site at least 15 min ahead of the scheduled time to allow sufficient time to set up laboratory supplies and ensure rapid transport of specimens to the laboratory after collection.

- Prepare and bring the following lab supplies:
  - 1 Tweezer
  - Wet ice 1 container
  - Blue Pads and Markers
  - 8 Pre-chilled 1.7mL Posi-click tubes
  - 2 scalpels
  - 10 slides of which 5 prelabeled

- Bring a PM worksheet with the corresponding PM identifier to the collection site.

3. Pre-collection Labeling

- Label 2 to 5 Posi-click tubes 1.7 ml
- Label 2 to 5 tubes 5ml
- Label with the following information:
  - Date of procedure
  - Specimen PMID

D. Tissue Sample Collection

1. While the tissue sample collection takes place:

- Record the following information on a PM worksheet:
  - Specimen PMID
  - Date of procedure
  - Type of specimen
  - Site
  - Number of specimen
  - Time of collection
  - Research team members

2. Once tissue sample is collected:

- DO NOT PLACE IN FORMALIN
- Transfer freshly collected tissue specimen(s) with tweezers into the pre-chilled tubes.
- Place tubes in wet ice.
- Dispose the needles or tweezers in the appropriate biohazard waste container(s).
- Bring the tissue specimen(s) to the Pathology Department as soon as possible.

E. Pathology evaluation

1. Labeling

- Label the Tissue Tek Cryomolds. Preparing more (2-4) cryomolds helps ensure that the team is prepared if additional cryomolds are needed.
- Label the cork to be placed atop of the Tek Cryomolds before freezing.
- Label 1 Superfrost plus slide per cryomold.
- Label with the following information:
    - Specimen PMID
    - 1-4 (this will help to identify each piece of tissue individually)

2. Gross examination

***NOTE: Gross examination will be done by a pathologist.**

- Take a picture of the specimen. Place small tissue cores in PBS buffer to prevent adhesion of tissue to glass slide. See image below.

- Report the gross examination:
    - Tissue type
    - Number of specimens
    - Size, weight of each specimen
    - Gross description
- Using sterile forceps, place the specimen in a cryomold prefilled with a drop of Tissue Tek™ OCT and pre labeled with the specimen PM

identifier (PMID). In case multiple biopsies are received, use only cryomold per core.

- Fill the cryomold with OCT medium ensuring no air bubbles are present.
- Place a labeled cork on top of the OCT and place the cryomold into the methylbutane/dry ice combination for no less than 60 seconds.
- Using the large Forceps remove the frozen tissue blocks from the methylbutane /dry ice combination and place in the -21 Cryostat.

- In case of a Bone Biopsy

- Each bone biopsy has to be cut in two parts: bone part (hard, whitish or pale in color) and marrow part (soft, reddish in color). See image below.

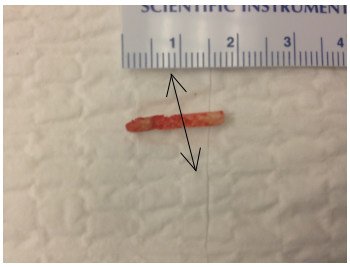

- The bone part must be placed into PBS medium for 20min before embedding.
- Place each part (marrow and bone) into a different cryomold prefilled with a drop of Tissue Tek™ OCT and pre labeled with the specimen PMID.

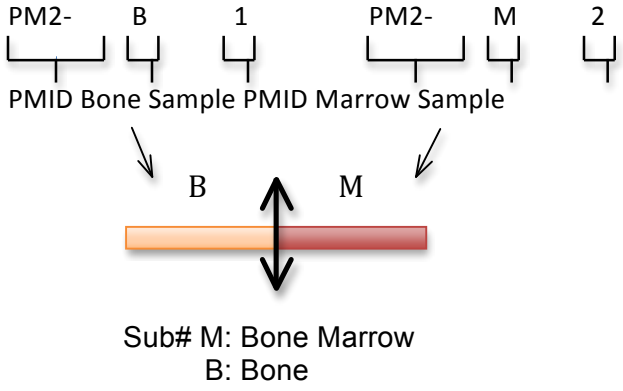

Sub# M: Bone Marrow
B: Bone

- Fill the cryomold with OCT medium ensuring no air bubbles are present.
- Place a labeled cork on top of the OCT and place the cryomold into the methylbutane /dry ice combination for no less than 60 seconds.
- Using the large Forceps remove the frozen tissue blocks from the methylbutane /dry ice combination and place in the -21 cryostat.

3. Procedure for tissue cutting

***NOTE: For safety purposes the Spec-Tec Cut Resistant Disposable Cut Gloves should be worn under the non-sterile glove for additional protection.**

- Using the Leica Slide Etcher. Print corresponding slides (PM1, #1-4) on the Superfrost Plus Slides for each tissue block that has been frozen.

***NOTE: All slides must remain at room temperature in order to ensure that the frozen tissue will adhere to the slide**.

- Place metal chucks in the -21 cryostat (1 chuck per tissue block).
- Cover the entire top of the chuck with the Tissue Tek OCT compound.
- Remove the frozen block from the Tissue Tek standard size cryomold and place the cork directly on to the OCT covered chuck.
- Allow 1 to 2 minutes for the OCT compound to fully freeze on the chuck before cutting.
- For H&E staining, the cryostat needs to have a thickness setting of 5 microns.
- Place a High Profile Disposable Blade in the blade holder and lock.
- Place metal chuck in block holder and adjust for cutting.
- Slowly level the frozen block with the blade and begin cutting.
- Cut block slowly until the tissue is fully faced.
- Cut the fully faced section and pull on to the cryostat's frozen block using a small pencil thin brush.
- Pick up tissue using the labeled Superfrost Plus Slide and place in the 24 count slide rack.
- Continue until all frozen blocks have been cut.
- Once all blocks have been cut, place 24 count slide rack in 100% alcohol – 200 Proof Pure Ethanol and prep slides for staining.

4. Procedure for slide staining

***NOTE: Slide Staining should always occur under a fume hood.**

- Stain 1 H&E slide per specimen.
- Fill the large container or bucket with water and place on the side of the Manual Hand staining Unit.
- Leave slide rack in 100% alcohol for 2/3 minutes.
- Remove 24 count slide rack from 100% alcohol and place in 95% alcohol for 2/3 minutes.
- Remove 24 count slide rack from 95% alcohol and rinse thoroughly in the large container or bucket filled with water.
- Place 24 count slide rack in hematoxylin for 45 seconds – Agitate gently.

- Remove from hematoxylin and place 24 count slide rack in water and rinse thoroughly to remove excess hematoxylin.
- Discard dirty water and refill the container or bucket with clean water.
- Place 24 count slide rack in Bluing Reagent (Lithium Carbonate) for 10 seconds – Agitate gently.
- Remove 24 count slide rack from Bluing Reagent (Lithium Carbonate) and rinse in water.
- Place 24 count slide rack in 95% alcohol for 5-10 seconds
- Remove from 95% alcohol and place 24 count slide rack in Eosin for 7-10 seconds.
- Remove 24 count slide rack from Eosin and blot on paper towel lightly once or twice to remove excess Eosin.
- Place 24 count slide rack in 95% alcohol for 5 seconds.
- After 5 seconds, remove from 95% alcohol and place in 100% alcohol for 5-10 seconds.
- Remove from 100% alcohol and place into a 2nd container filled with 100% alcohol for 5-10 seconds.
- After 5-10 seconds, remove the 24 count slide rack and place it into a 3rd container filled with 100% alcohol for 5-10 seconds.
- Remove the 24 count slide rack from the 3rd container filled with 100% alcohol and blot on a paper towel to drain excess alcohol.
- After draining excess alcohol onto the paper towel, place the 24 count slide rack into xylene for 10 seconds.
- After 10 seconds, remove from xylene and place in a 2nd container filled with xylene for 10 seconds.
- After 10 seconds in the 2nd container of xylene, the staining process is complete.
- To cover slip the slides, leave the 24 count slide rack in xylene and remove slides individually.
- Place 1 to 2 drops of Thermo Scientific Cytoceal – XYL on the tissue that is on the slide.
- Take 1 microscope cover glass and gently place it over the tissue that is on the slide.
- Blot the slide and cover glass on paper towel to remove any excess Cytoceal that may be around the edges of the slide.
- Place slide in a 20 count slide holder booklet and let dry.
- Continue this until all slides are cover slipped.

5. Pathology evaluation

- After slides are dried, a pathologist reviews the H&E slides. At this point, if any additional slides need to be cut, instruction will be given to do so.

- Evaluate size of tissue, confirm the presence of tumor and evaluate tumor content (percentage of tumor involvement) for each block.
- Note presence of necrosis and/or normal tissue if present.
- Document above information in pathology report.
- If multiple blocks/passes have been analyzed, document best blocks that should be used for analysis in pathology report- these are blocks with the highest tumor content.
- Representative images are taken from H&E slides.

6. Procedure to convert frozen tissue into formalin-fixed paraffin-embedded (FFPE) tissue

- After pathology evaluation of frozen material, the pathologist determines which cryomold is converted to FFPE if the amount of frozen tissue is enough for processing. FFPE tissue is used for clinical documentation (when applicable) and to perform subsequent assays (e.g. IHC, FISH).

- Let cryomold thaw for approx. 2 minutes until OCT starts to melt.
- Separate excess OCT from tissue.
- Wrap tissue in lens paper and place it plastic cassette.
- Place cassette in formalin.

7. Scanning slides

- Send H&E stained slides for APERIO Scanning.

F. Specimen Storage

1. Specimen Storage

- After all slides have been reviewed
  - Take all metal chucks out of the cryostat and place under the hood or on the bench.
  - Remove frozen blocks from metal chuck using forceps.
  - Place frozen blocks in the plastic zip lock bag that was labeled with the PM Identifier and the date.
  - Transfer cryopreserved labeled specimen(s) to an -80°C freezer at the designated floor.

2. Information uploaded into the LIMS

- Record the following information into the LIMS system in the Tissue Processing file:
  - PM number

- Date of procedure
- Number of specimens
- Site
- Time of collection
- Time of freezing
- Diagnosis
- Representative H&E images of each specimen.
- Date/time of specimen(s) placed at -80°C.
- Location of the specimen.

Precision Medicine Program at WCMC

STANDARD OPERATING PROCEDURES (SOP)

Tissue Specimen Collection

PM#….

General information

Date of procedure …/…/…

Specimen PMID PM.....

Type of specimen …….

Research team …….

Pathologist …….

Technician …….

	Sample 1	Sample 2	Sample 3	Sample 4
Time of collection				
Type of specimen				
Site				
Size (mm)				
Time of freezing				
Diagnosis				

Institute for Precision Medicine Report

Patient ID: **Diagnosis:** Metastatic urothelial carcinoma **Report date:** Jun. 05, 2014

CLINICAL INFORMATION

Patient ID:
Physician:
Diagnosis: Metastatic urothelial carcinoma
Site: Inguinal mass
Specimen IDs (case/control)

Sample type (case/control): Frozen Tissue / Blood
Sample collected (case/control): (12/20/2013) / (11/25/2013)
Sample received (case/control): (1/15/2014) / (1/15/2014)
Neoplastic content: 63.0%

CASE IMAGES

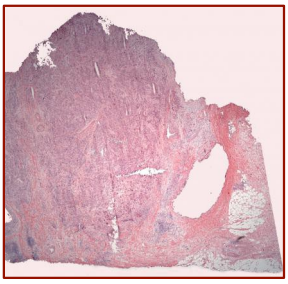
H&E 2x

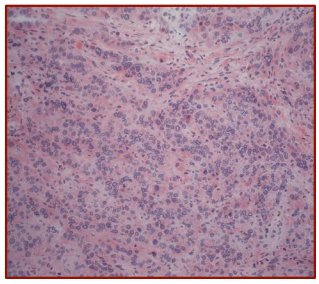
H&E 10x

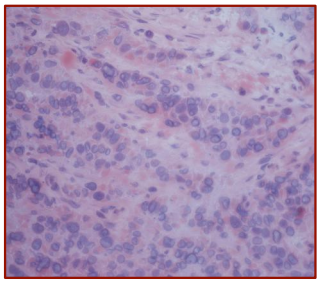
H&E 20x

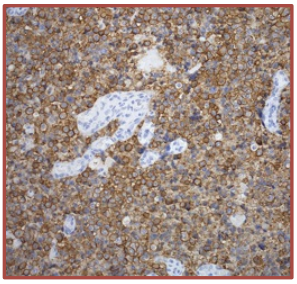
Her2 20x

RESULTS

GENOMIC ALTERATIONS: Summary

Somatic alterations in clinically relevant genes

A set of 50 clinically relevant genes was investigated. 3 alterations were found in these genes (listed below).

Somatic alterations of unknown significance in known cancer genes

A set of 508 known cancer genes was investigated. 12 alterations in these cancer associated genes were found (listed below).

Somatic alterations of unknown significance

194 gene(s) with point mutations or indels and 131 copy number alteration(s) were found (listed below).

Clinically relevant genomic alterations

These alterations occur in genes that are deemed clinically relevant because: they are targets of drugs, they confer resistance or susceptibility to treatment, or for other clinically relevant reasons (see Appendix).

Gene name	FDA approved drugs with indication (if any)	Interpretation
ERBB2 Amplification	Breast_Cancer:Trastuzumab	ERBB2 (HER2) amplification and over-expression are associated with sensitivity to Trastuzumab, an anti-HER2 antibody.

Gene name	FDA approved drugs with indication (if any)	Interpretation
FGFR1 Amplification	none	FGFR1 amplification is associated with poor survival in patients with resected squamous cell lung cancer (Kim et al, 2012, JCO). FGRF1 amplification may be associated with sensitivity to the multitargeted tyrosine kinase inhibitor pazopanib(Liao et al, 2013, Cancer Res).
KIT p.E76K VAF:36.1%	none	In AML, presence of exon 17 mutations in KIT may confer an adverse prognosis or increased relapse rate.

VAF: variant allele frequency

Genomic alterations of unknown significance in cancer genes

These alterations occur in genes that are cancer associated, but their impact on the disease is unknown (see Appendix).

Copy number alterations

Gene name	Description	Classification of alteration	Altered region
NKX2-1	NK2 homeobox 1	FOCAL AMPLIFICATION	chr14:36190972-36989294
APC	adenomatous polyposis of the colon gene	LARGE SCALE DELETION	chr5:99725313-118965496

Genomic coordinates are based on human reference GRC37/hg19. Large scale alterations involve at least 50 genes.

Somatic mutations and indels

Gene name	Gene description	Classification	Reference Allele	Tumor Allele 1	Tumor Allele 2	AA change	Tumor (Normal) read depth	Tumor VAF
TSC1 chr9:135776991	tuberous sclerosis 1 gene	nonsense	G	G	A	p.Q830*	112 (109)	67.9%
TP53 chr17:7578276	tumor protein p53	nonsense	G	G	A	p.Q192*	73 (72)	67.1%
TPR chr1:186315414	translocated promoter region	nonsense	C	C	A	p.E984*	160 (209)	28.7%
FNBP1 chr9:132691939	formin binding protein 1 (FBP17)	missense	C	C	G	p.E184Q	43 (37)	72.1%
BRIP1 chr17:59858315	BRCA1 interacting protein C-terminal helicase 1	missense	G	G	C	p.Q561E	137 (91)	32.8%
ITK chr5:156638344	IL2-inducible T-cell kinase	missense	G	G	C	p.E97Q	70 (70)	38.6%
FNBP1 chr9:132687316	formin binding protein 1 (FBP17)	missense	C	C	T	p.R304K	51 (44)	52.9%
ATM chr11:108099937	ataxia telangiectasia mutated	missense	G	G	C	p.E73Q	87 (87)	27.6%
KTN1 chr14:56116499	kinectin 1 (kinesin receptor)	missense	C	C	G	p.S791C	47 (48)	44.7%
BCL9 chr1:147094190	B-cell CLL/lymphoma 9	missense	C	C	G	p.S1007C	118 (46)	28.0%

AA: amino-acid; VAF: variant allele frequency; Genomic coordinates are based on human reference GRC37/hg19 and are 1-based.

Institute for Precision Medicine Report

Patient ID: PM137 **Diagnosis:** Metastatic urothelial carcinoma **Report date:** Jun. 05, 2014

Genomic alterations of unknown significance

These alterations are not known to have any effect on the disease, but are here reported in the event that in the future progress in scientific knowledge could determine their role (see Appendix).

Somatic mutations and indels

Gene name	Classification	Reference Allele	Tumor Allele 1	Tumor Allele 2	AA change	Tumor (Normal) read depth	Tumor VAF
KCNS1 chr20:43727084	missense	G	G	T	p.F110L	202 (158)	75.2%
CCDC180 chr9:100076787	missense	G	G	A	p.E235K	134 (228)	59.0%
ZSWIM5 chr1:45553827	nonsense	G	G	A	p.R227*	152 (180)	61.8%
IGFL3 chr19:46627175	missense	G	G	C	p.H107D	286 (289)	39.9%
LOC729020 chr10:105006197	missense	G	G	C	p.E148Q	113 (176)	62.8%
C6 chr5:41181647	missense	C	C	G	p.D248H	114 (103)	72.8%
FLG chr1:152284994	missense	G	G	A	p.S790L	181 (219)	43.1%
POLR3G chr5:89802391	missense	G	G	C	p.E162Q	93 (116)	69.9%
RBPMS chr8:30407088	missense	C	C	T	p.A200V	208 (231)	37.5%
GPR19 chr12:12814865	missense	G	G	C	p.F173L	141 (200)	44.7%
ZNF629 chr16:30794396	missense	G	G	C	p.I418M	148 (144)	52.0%
ADAT1 chr16:75646731	missense	C	C	T	p.E152K	124 (208)	45.2%
TMEM132C chr12:129190507	missense	T	T	C	p.I998T	121 (104)	63.6%
FAM49A chr2:16742519	missense	C	C	T	p.E181K	93 (112)	64.5%
CALML6 chr1:1847158	missense	C	C	G	p.Q21E	260 (193)	36.9%
BRD7 chr16:50362640	missense	C	C	T	p.R343K	78 (130)	61.5%
GCN1L1 chr12:120600736	missense	C	C	G	p.R693S	163 (151)	46.0%
MAP4K3 chr2:39494344	missense	C	C	G	p.Q673H	84 (79)	73.8%
RP1L1 chr8:10480334	nonsense	G	G	A	p.Q127*	97 (232)	43.3%

Institute for Precision Medicine Report

Patient ID: **Diagnosis:** Metastatic urothelial carcinoma **Report date:** Jun. 05, 2014

Gene name	Classification	Reference Allele	Tumor Allele 1	Tumor Allele 2	AA change	Tumor (Normal) read depth	Tumor VAF
SYNGAP1 chr6:33400544	missense	C	C	T	p.R157C	25 (32)	36.0%
MEX3A chr1:156047072	missense	G	G	A	p.T286M	60 (30)	30.0%
RAI1 chr17:17700200	frameshift deletion	C	-	-	p.A1313_fs	27 (40)	81.5%
RPRML chr17:45055758	frameshift deletion	AC	-	-	p.F205_fs	16 (4)	81.2%
HMCN1 chr1:185834937	frameshift insertion	-	+A	-	p.E188_fs	34 (30)	38.2%
TMEM87B chr2:112832536	inframe deletion	AAT	-	AAT	p.S166_nofs	58 (26)	39.7%
WWC1 chr5:167881030	inframe deletion	GGA	-	-	p.V861_nofs	38 (34)	81.6%

AA: amino-acid; VAF: variant allele frequency; Genomic coordinates are based on human reference GRC37/hg19 and are 1-based.

Copy number alterations

Location (Chr:Start-End)	Type	Number of genes	Number of exons	Gene names (if less than 3)
chr1:145,460,153-147,806,639	FOCAL AMPLIFICATION	37	191	too many to show
chr1:149,783,705-151,774,554	LARGE SCALE AMPLIFICATION	74	604	too many to show
chr1:158,906,831-161,336,258	LARGE SCALE AMPLIFICATION	70	538	too many to show
chr1:161,337,643-161,495,470	FOCAL AMPLIFICATION	3	9	C1orf192; HSPA6; FCGR2A
chr1:161,495,811-161,600,916	FOCAL AMPLIFICATION	6	13	too many to show
chr1:161,641,203-162,829,341	FOCAL AMPLIFICATION	18	119	too many to show
chr1:169,356,326-169,930,280	FOCAL AMPLIFICATION	11	126	too many to show
chr1:9,416,296-9,667,729	FOCAL AMPLIFICATION	4	16	too many to show
chr10:5,415,925-5,442,849	FOCAL AMPLIFICATION	2	4	TUBAL3; UCN3
chr10:5,442,978-5,683,827	FOCAL AMPLIFICATION	5	20	too many to show
chr10:5,684,514-5,694,918	FOCAL AMPLIFICATION	1	4	ASB13
chr11:19,372,528-31,287,099	FOCAL AMPLIFICATION	39	354	too many to show
chr11:31,312,295-34,654,166	FOCAL AMPLIFICATION	30	308	too many to show
chr11:34,664,224-36,692,824	FOCAL AMPLIFICATION	17	127	too many to show
chr11:4,976,058-4,976,358	FOCAL DELETION	1	2	OR51A2
chr11:57,068,042-57,509,637	FOCAL AMPLIFICATION	20	141	too many to show
chr11:73,814,421-75,188,720	FOCAL DELETION	23	192	too many to show
chr12:33,529,799-33,579,250	FOCAL AMPLIFICATION	1	9	SYT10
chr12:50,642,473-51,693,443	FOCAL AMPLIFICATION	16	161	too many to show

Location (Chr:Start-End)	Type	Number of genes	Number of exons	Gene names (if less than 3)
chrX:24,082,383-24,089,758	FOCAL DELETION	1	4	EIF2S3
chrX:74,961,284-75,649,759	FOCAL AMPLIFICATION	4	12	too many to show
chrX:76,139,740-77,395,081	FOCAL AMPLIFICATION	9	106	too many to show
chrX:77,528,324-78,622,655	FOCAL AMPLIFICATION	7	15	too many to show
chrX:80,370,441-80,552,708	FOCAL AMPLIFICATION	2	12	HMGN5; SH3BGRL
chrX:91,456,412-91,873,596	FOCAL AMPLIFICATION	1	5	PCDH11X
chrX:92,927,541-103,080,410	LARGE SCALE AMPLIFICATION	67	351	too many to show

Genomic coordinates are based on human reference GRC37/hg19. Large scale alterations involve at least 50 genes.

Method

Genomic DNA was extracted from macrodissected formalin-fixed paraffin-embedded (FFPE) tumor, or cored frozen, OCT-embedded tumor and peripheral blood lymphocytes of the patient's specimens using the Promega Maxwell 16 MDx. Estimation of tumor content is based on analysis of the sequencing data using CLONET version 0.3 [1]. Sequencing was performed using Illumina HiSeq 2500 (2x100bp). A total of 21,522 genes were analyzed with an average coverage of 84x (81x) using Agilent HaloPlex. 71,073,768 (68,658,329) short reads were aligned to GRC37/hg19 reference using BWA [2] and processed accordingly to Whole Exome Sequencing Test for Cancer - ExaCT1 - pipeline v0.9. The capture efficiency is 84.08% (84.25%).
NB: numbers in parentheses refer to the control sample.

1. Baca, S, Prandi D. et al. Punctuated evolution of prostate cancer genomes. Cell 2013 Apr 25;153(3):666-77. doi: 10.1016/j.cell.2013.03.021.
2. Li, Heng, and Durbin Richard. Fast and Accurate Long-read Alignment with Burrows-Wheeler Transform. Bioinformatics 2010;26(5)(March 1):589–595. doi:10.1093/bioinformatics/btp698

Appendix

Clinically relevant genes: These genes are deemed clinically relevant because: they are targets of drugs, they confer resistance or susceptibility to treatment, or for other clinically relevant reasons. As the scientific knowledge increases, this list will be updated accordingly. A total of 93 alterations in 50 genes are considered in this report.

Somatic alterations of unknown significance in cancer genes or in other genes: These genes may not be related to the disease. Current scientific knowledge cannot determine the impact of these alterations on the disease. These genes are included herein in the event they become clinically relevant as our knowledge increases. Specifically, this report considers 508 cancer genes that are listed in the section 'Genomic alterations of unknown significance in cancer genes'.

Alterations are not listed in ranked order: The order of the alterations reported as clinically relevant or of unknown significance is **not** associated with predicted effect on tumor development, progression, or resistance to treatment.

Treatement decisions: The treating physician is responsible to select the most appropriate course of treatment. Decision making about therapy should not be based solely on the information contained in this report.

List of clinically relevant and known cancer genes:
ABL1; ABL2; AKT1; AKT2; AKT3; ALK; AR; AURKA; BCL2; BRAF; BRCA1; BRCA2; CD79B; CDK4; CDK6; CDKN2A; CEBPA; CRKL; DNMT3A; EGFR; ERBB2; ERBB3; ERBB4; FGFR1; FGRF1; FGFR2; FGFR3; FGFR4; FLT3; GNA11; GNAQ; GNAS; HRAS; IDH1; IDH2; IKZF1; JAK2; KIT; KRAS; MAP2K1; MAP2K2; MCL1; MET; NRAS; PDGFRA; PIK3CA; PTCH1; PTEN; SMO; TSC1; ACSL3; AF15Q14; AF1Q; AF3p21; AF5q31; AKAP9; ALDH2; ALO17; APC; ARHGEF12; ARHH; ARID1A; ARID2; ARNT; ASPSCR1; ASXL1; ATF1; ATIC; ATM; ATRX; AXIN1; BAP1; BCL10; BCL11A; BCL11B; BCL3; BCL5; BCL6; BCL7A; BCL9; BCOR; BCR; BHD; BIRC3; BLM; BMPR1A; BRD3; BRD4; BRIP1; BTG1; BUB1B; C12orf9; C15orf21; C15orf55; C16orf75; C2orf44; CAMTA1; CANT1; CARD11; CARS; CBFA2T1; CBFA2T3; CBFB; CBL; CBLB; CBLC; CCDC6; CCNB1IP1; CCND1; CCND2; CCND3; CCNE1; CD273; CD274; CD74; CD79A; CDH1; CDH11; CDK12; CDKN2a(p14);

CDKN2C; CDX2; CEP1; CHCHD7; CHEK2; CHIC2; CHN1; CIC; CIITA; CLTC; CLTCL1; CMKOR1; CNOT3; COL1A1; COPEB; COX6C; CREB1; CREB3L1; CREB3L2; CREBBP; CRLF2; CRTC3; CTNNB1; CYLD; D10S170; DAXX; DDB2; DDIT3; DDX10; DDX5; DDX6; DEK; DICER1; DNM2; DUX4; EBF1; ECT2L; EIF4A2; ELF4; ELK4; ELKS; ELL; ELN; EML4; EP300; EPS15; ERCC2; ERCC3; ERCC4; ERCC5; ERG; ETV1; ETV4; ETV5; ETV6; EVI1; EWSR1; EXT1; EXT2; EZH2; EZR; FACL6; FAM22A; FAM22B; FAM46C; FANCA; FANCC; FANCD2; FANCE; FANCF; FANCG; FBXO11; FBXW7; FCGR2B; FEV; FGFR1OP; FH; FHIT; FIP1L1; FLI1; FLJ27352; FNBP1; FOXL2; FOXO1A; FOXO3A; FOXP1; FSTL3; FUBP1; FUS; FVT1; GAS7; GATA1; GATA2; GATA3; GMPS; GOLGA5; GOPC; GPC3; GPHN; GRAF; H3F3A; HCMOGT-1; HEAB; HERPUD1; HEY1; HIP1; HIST1H3B; HIST1H4I; HLF; HLXB9; HMGA1; HMGA2; HNRNPA2B1; HOOK3; HOXA11; HOXA13; HOXA9; HOXC11; HOXC13; HOXD11; HOXD13; HRPT2; HSPCA; HSPCB; IGH@; IGK@; IGL@; IL2; IL21R; IL6ST; IL7R; IRF4; IRTA1; ITK; JAK1; JAK3; JAZF1; JUN; KCNJ5; KDM5A; KDM5C; KDM6A; KDR; KIAA1549; KIF5B; KLF4; KLK2; KTN1; LAF4; LASP1; LCK; LCP1; LCX; LHFP; LIFR; LMO1; LMO2; LPP; LRIG3; LYL1; MADH4; MAF; MAFB; MALT1; MAML2; MAP2K4; MAX; MDM2; MDM4; MDS1; MDS2; MECT1; MED12; MEN1; MITF; MKL1; MLF1; MLH1; MLL; MLL2; MLL3; MLLT1; MLLT10; MLLT2; MLLT3; MLLT4; MLLT6; MLLT7; MN1; MPL; MSF; MSH2; MSH6; MSI2; MSN; MTCP1; MUC1; MUTYH; MYB; MYC; MYCL1; MYCN; MYD88; MYH11; MYH9; MYST4; NACA; NBS1; NCOA1; NCOA2; NCOA4; NDRG1; NF1; NF2; NFE2L2; NFIB; NFKB2; NIN; NKX2-1; NONO; NOTCH1; NOTCH2; NPM1; NR4A3; NSD1; NT5C2; NTRK1; NTRK3; NUMA1; NUP214; NUP98; OLIG2; OMD; P2RY8; PAFAH1B2; PALB2; PAX3; PAX5; PAX7; PAX8; PBRM1; PBX1; PCM1; PCSK7; PDE4DIP; PDGFB; PDGFRB; PER1; PHF6; PHOX2B; PICALM; PIK3R1; PIM1; PLAG1; PML; PMS1; PMS2; PMX1; PNUTL1; POT1; POU2AF1; POU5F1; PPARG; PPP2R1A; PRCC; PRDM1; PRDM16; PRF1; PRKAR1A; PRO1073; PSIP2; PTCH; PTPN11; RAB5EP; RAC1; RAD51L1; RAF1; RALGDS; RANBP17; RAP1GDS1; RARA; RB1; RBM15; RECQL4; REL; RET; RNF43; ROS1; RPL10; RPL22; RPL5; RPN1; RUNDC2A; RUNX1; RUNXBP2; SBDS; SDC4; SDH5; SDHB; SDHC; SDHD; SEPT6; SET; SETBP1; SETD2; SF3B1; SFPQ; SFRS3; SH2B3; SH3GL1; SIL; SLC34A2; SLC45A3; SMARCA4; SMARCB1; SMARCE1; SOCS1; SOX2; SRGAP3; SRSF2; SS18; SS18L1; SSH3BP1; SSX1; SSX2; SSX4; STAT3; STK11; STL; SUFU; SUZ12; SYK; TAF15; TAL1; TAL2; TCEA1; TCF1; TCF12; TCF3; TCF7L2; TCL1A; TCL6; TERT; TET2; TFE3; TFEB; TFG; TFPT; TFRC; THRAP3; TIF1; TLX1; TLX3; TMPRSS2; TNFAIP3; TNFRSF14; TNFRSF17; TNFRSF6; TOP1; TP53; TPM3; TPM4; TPR; TRA@; TRAF7; TRB@; TRD@; TRIM27; TRIM33; TRIP11; TSC2; TSHR; TTL; U2AF1; USP6; VHL; VTI1A; WAS; WHSC1; WHSC1L1; WIF1; WRN; WT1; WTX; WWTR1; XPA; XPC; XPO1; YWHAE; ZNF145; ZNF198; ZNF278; ZNF331; ZNF384; ZNF521; ZNF9; ZRSR2.

Disclaimer

The information here provided is for investigational use only. We do not exclude the possibility of other genomic alterations present that could not have been identified for biological or technical reasons.
Gene variants present in less than 20% of cells may not be detected by this test.

This method has not been cleared by the FDA. The analytical performance characteristics have been determined by the Institute for Precision Medicine/New York Hospital Laboratories.

The report was generated at 20:18:51 EDT - Jun 5, 2014; based on version 8567f8e of software IPM-reportGenerator.

eReferences

1. Prandi D, Baca SC, Romanel A, Barbieri CE, Mosquera J, Fontugne J, et al. Unraveling the clonal hierarchy of somatic genomic aberrations. Genome Biol. 2014;15:439.
2. Campagne F, Dorff KC, Chambwe N, Robinson JT, Mesirov JP. Compression of structured high-throughput sequencing data. PLoS One. 2013;8:e79871.
3. Demichelis F, Greulich H, Macoska JA, Beroukhim R, Sellers WR, Garraway L, et al. SNP panel identification assay (SPIA): a genetic-based assay for the identification of cell lines. Nucleic Acids Res. 2008;36:2446-56.
4. Baca SC, Prandi D, Lawrence MS, Mosquera JM, Romanel A, Drier Y, et al. Punctuated evolution of prostate cancer genomes. Cell. 2013;153:666-77.
5. Jiang Y, Soong TD, Wang L, Melnick AM, Elemento O. Genome-wide detection of genes targeted by non-Ig somatic hypermutation in lymphoma. PLoS One. 2012;7:e40332.
6. Li H, Handsaker B, Wysoker A, Fennell T, Ruan J, Homer N, et al. The Sequence Alignment/Map format and SAMtools. Bioinformatics. 2009;25:2078-9.
7. Li H, Durbin R. Fast and accurate short read alignment with Burrows-Wheeler transform. Bioinformatics. 2009;25:1754-60.
8. McKenna A, Hanna M, Banks E, Sivachenko A, Cibulskis K, Kernytsky A, et al. The Genome Analysis Toolkit: a MapReduce framework for analyzing next-generation DNA sequencing data. Genome Res. 2010;20:1297-303.
9. Wang J, Mullighan CG, Easton J, Roberts S, Heatley SL, Ma J, et al. CREST maps somatic structural variation in cancer genomes with base-pair resolution. Nat Methods. 2011;8:652-4.
10. Ran FA, Hsu PD, Wright J, Agarwala V, Scott DA, Zhang F. Genome engineering using the CRISPR-Cas9 system. Nature protocols. 2013;8:2281-308.
11. Hsu PD, Scott DA, Weinstein JA, Ran FA, Konermann S, Agarwala V, et al. DNA targeting specificity of RNA-guided Cas9 nucleases. Nature biotechnology. 2013;31:827-32.
12. Beltran H, Rickman DS, Park K, Sboner A, MacDonald TY, Wang Y, et al. Molecular Characterization of Neuroendocrine Prostate Cancer and Identification of New Drug Targets. Cancer Discovery. 2011;1:487-95.